4^{th} SEMESTER MCE

DRIFT COMPENSATION OF STATE OF THE ART STEERING SYSTEM FOR LARGE COMMERCIAL TRACTORS

31^{st} of May 2024

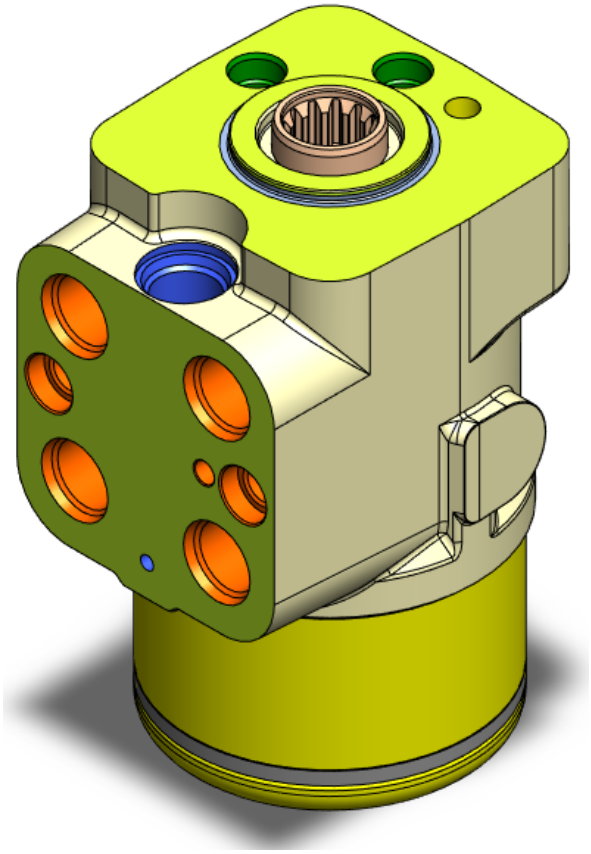

Mechatronic Control Engineering, MCE4-1027
Department of Energy Technology, Aalborg University

AALBORG UNIVERSITET
STUDENTERRAPPORT

Department of Energy Technology
Mechatronic Control Engineering
Pontoppidanstræde 111
9220 Aalborg Øst

Title:
Drift compensation of state of the art steering system for large commercial tractors

Project:
4^{th} semester MCE

Project period:
5^{th} of February to 31^{st} of May 2024

Project group:
MCE4-1027

Email:
amort19@student.aau.dk

Supervisor:
Henrik Clemmensen Pedersen

Company supervisor:
Emil Nørregård Olesen

Number of pages:
33

Number of appendices:
11

Finish date:
31^{st} of May 2024

Participants:

Alexander Belusa Mortensen

Abstract:

In agricultural vehicles large forces are required to operate the steering axis because of the weight of the vehicles as well as the terrain they operate in. For this purpose hydraulic solutions are applied due to the forces that they are capable of delivering. However, in hydraulics the leakage must always be considered. This report models such leakages in the gearset of Danoss' OSP unit. These leakages cause a drift on the steering wheel of the vehicle which Danfoss are interested in reducing. Modelling the leakages and applying them to a nonlinear model, can be used to further understand what causes these leakages have on the system and could prove a valuable tool to find ways to reduce the leakage. Due to issues with the model the focus of this report has been analysing the OSP hydraulic system to find the cause of the modelling errors.

Preface

This project has been written as part of the curriculum for the 4th semester of the Mechanical Control Engineering Master at Aalborg University. The student would like to thank company supervisor Emil Nørregård Olesen and supervisor at AAU Henrik Clemmensen Pedersen for their guidance throughout the project. The in-text citations use the Vancouver reference style, [Reference number to a source in the Bibliography]. The first time an abbreviation is used, the word will be written, followed by the abbreviation in parenthesis. This semester project was written in LATEX with the model made in MATLAB and simulations were done in MATLAB Simulink. Drawings and diagrams were made in MATLAB and Inkscape

Aalborg University, May 31, 2024

Nomenclature

Symbol	Definition	Unit
β_{eff}	Bulk Modulus	$[Pa]$
δ	Gap height	$[m]$
θ	Angle	[°]
μ	Friction Constant	[-]
τ	Torque	$[N\,m]$
φ	Angle Difference Between Spool and Sleeve	[°]
A	Area	$[m^2]$
a	Constant	[-]
B	Viscous Friction	$[\frac{N\,s}{m}]$
b	Constant	[-]
C	Coulomb Friction	$[\frac{N}{m}]$
C	Discharge Coefficient	[-]
C	Leakage Coefficient	[-]
c	Constant	[-]
D	Diameter	$[m]$
D	Displacement	$[\frac{cm^3}{rev}]$
F	Force	$[N]$
k	Constant	[-]
L	Length	$[m]$
m	Mass	$[kg]$
p	Pressure	$[Pa]$
Q	Flow	$[\frac{L}{min}]$
V	Volume	$[m^3]$
x	Position	$[m]$
$\dot{x}$	Velocity	$[\frac{m}{s}]$
$\ddot{x}$	Acceleration	$[\frac{m}{s^2}]$

Subscripts	Definition
μ	Friction coefficient
A	A-side of Cylinder
B	B-side of Cylinder
d	Discharge
ext	External
hyd	Hydraulic
Le	Leakage
p	Piston
p	Pump
s	Spring
SL	Sleeve
SP	Spool
ST	Steer
T	Tank
v	Valve

Acronym	Definition
LS	Load Sensing
MSD	Mass Spring Damper System
OSP	Orbital Steering Pump

Contents

1 Introduction

The operation of agricultural vehicles includes the ability to steer the direction of the wheel. To do so for agricultural vehicles requires high-power solutions since purely mechanical servo steering, as used in cars, is not capable of maneuvering such loads. Therefore hydraulic power steering is an easy and flexible way to operate these vehicles. Danfoss' Orbital Steering Pump (OSP), can be used to control the hydraulic cylinders with high precision, while also maintaining operator comfort. The new state of the art OSPS LSRS unit was modelled in an earlier project [1] in which it was found that leakage resulted in the steering unit experiencing a drift issue such that the steering wheel would find a different position in some cases. This phenomenon can be seen in Figure 1.1. Here the cylinder position goes back to 0, however, the steering wheel angle ends up being offset by 20 degrees.

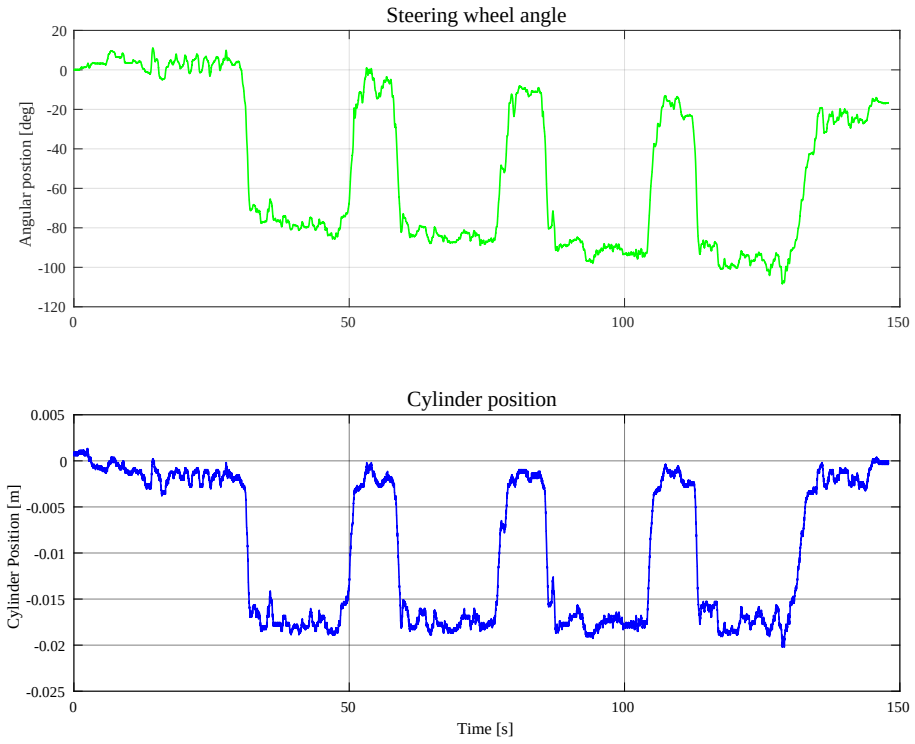

Figure 1.1. Drift test showcasing steering wheel angle not maintaining its neutral position.

It is of interest to the customer and therefore Danfoss to avoid this drift issue as it reduces operator steering comfort as this can be directly felt on the steering wheel. This can also be an annoyance for operators utilizing a knob on the steering wheel as the steering wheel position will not be consistent.
Based on this, the project seeks to further examine the drift on the OSP the initial problem is therefore:

What is the root cause of the drift on the OSP and can this be represented correctly in a model.

Problem Analysis 2

2.1 System Description

In Figure 2.1 the general view of a standard Ackermann steering setup is shown where the OSP is seen implemented in the front axis of a high-load agricultural vehicle. Here the OSP controls the flow to the cylinders, this hydraulic system functions as servo steering for the agricultural vehicle.

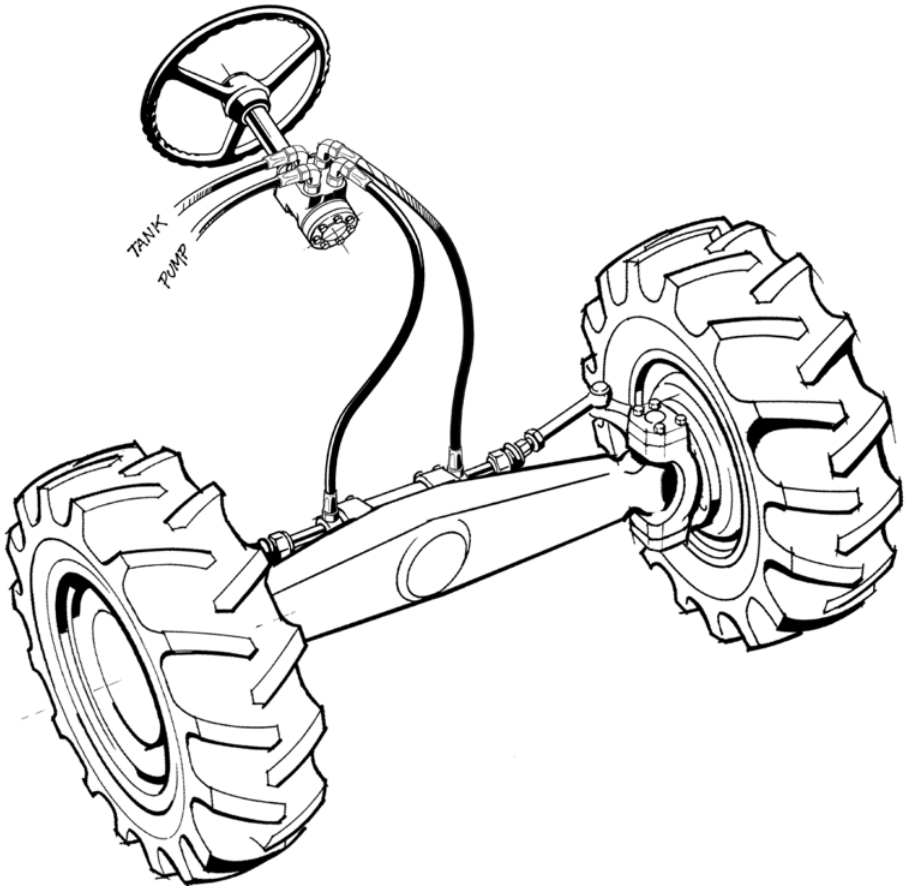

Figure 2.1. Front axis connection with OSP. [2].

The OSP is coupled with the steering wheel such that rotating the steering wheel will actuate the cylinders resulting in the wheels turning in the desired direction and with a linear relationship between steering wheel movement and cylinder movement. An exploded view of the OSP is shown in Figure 2.2.

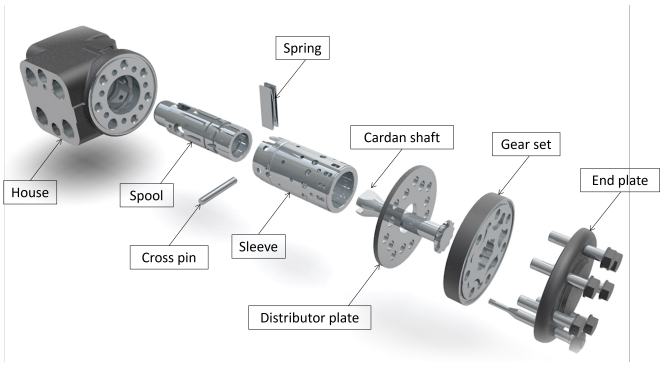

Figure 2.2. Exploded view of the OSP unit [2].

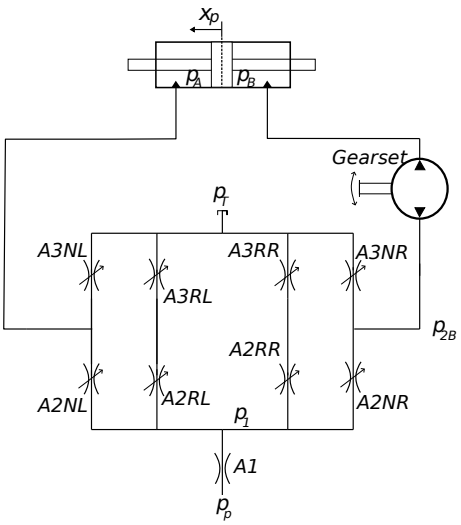

Figure 2.3. Simplified hydraulic schematic

The OSP unit is controlled by the vehicle's steering wheel. The house is connected to the pump and tank of the hydraulic system as well as the left and right side cylinders. As the operator rotates the steering wheel it is mechanically connected to the spool, thus the spool will be rotated equally as much. The orifices of the hydraulic system depend on the holes of the spool, sleeve and house lining up. In the OSPS unit the sleeve and spool are connected through a spring such that the rotation of the sleeve lags the rotation of the spool. It is this angular difference that determines which areas open and how far they open which is shown by the area curves in Figure 4.1. The cardan shaft interacts with the gearset works such that rotating the steering wheel will result in the OSP meting out fluid proportional to the rate of the steering wheel rotation. A simplified hydraulic schematic can be seen in Figure 2.3. The areas A2RL, A3RL, A2RR and A3RR are open during no and small adjustments of the steering wheel. These areas functions in a way that Danfoss calls reaction mode steering, with reaction mode featuring self alignment of the vehicle as well as replicating bumps in the terrain to the steering wheel.
During a clockwise rotation the areas A2NR and A3NL open and the gearset pumps fluid from p_{2B} to p_B, which then moves the cylinder towards the left. Counter-clockwise rotation results in A2NL and A3NR opening as well as the gearset pumping fluid from p_B to p_{2B}, which then moves the cylinder towars the left. Figure 2.4 shows how a left rotation on the steering wheel will pump fluid through the gearset.

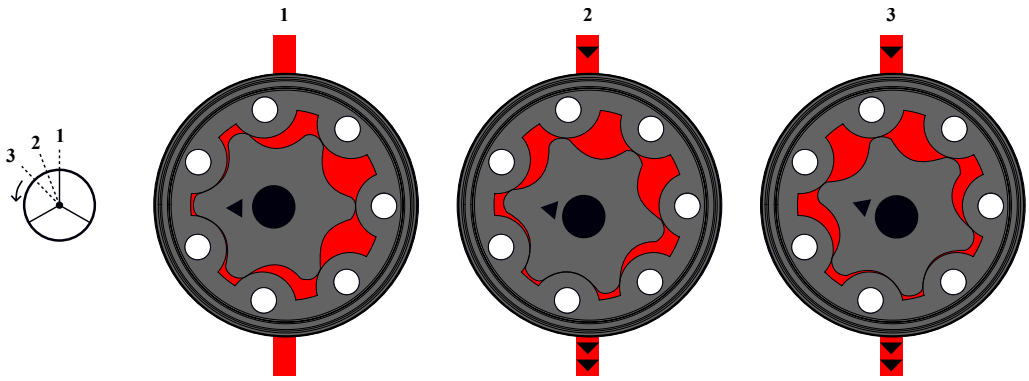

Figure 2.4. Left rotation of the steering wheel illustrated on gearset [3].

While turning the steering wheel the spool will follow the steering wheel rotation directly, while the sleeve will lag behind as the spool and sleeve are connected through the spring. The Mass-Spring-Damper system between the spool and sleeve is disclosed in [1] and will be mentioned in Section 4.1.

Figure 2.5 shows the system in neutral state, meaning no rotation on the steering wheel. In this scenario the fluid from the pump cannot enter the OSP seen in (1) resulting in low pressure throughout the system. The load sensing (LS) system utilize the pressure as seen in (2), resulting in the LS system ensuring that the pressure going into (1) does not result in a pressure build up. Furthermore (4) and (6) functions as the reaction mode in the system, in this scenario these function as small orifices between the LS pressure in (2) and the tank (7). Ensuring that the pressure is low and thus the losses of the system are minimal, as mentioned earlier these are open during no or small rotations.

Figure 2.6 shows the system during a left rotation. Here fluid from the pump goes through the house and sleeve and into the spool (1). From here the fluid follows the channels along the sleeve, and as the OSP is rotated to the left it can be seen that (5) functions as the orifice A2NL, allowing fluid into the left side of the cylinder. This results in the cylinder moving right and thus turning the wheels to the left as seen in the steering geometry sketch on the figure. The fluid from the right side of the cylinder is then pushed into the gearset which is turning due to the rotation of the steering wheel, thus pushing fluid to (3) which function as the A3NR orifice and then connects to the tank. Here the LS system utilizes the pressure from (2) to ensure that the pump gives enough pressure to move the cylinder, however when this happens pressure will stop increasing in (2) and the LS system then ensures this pressure level. In this case (6) and (4) which is the reaction mode has no function, as the steering wheel is rotated.

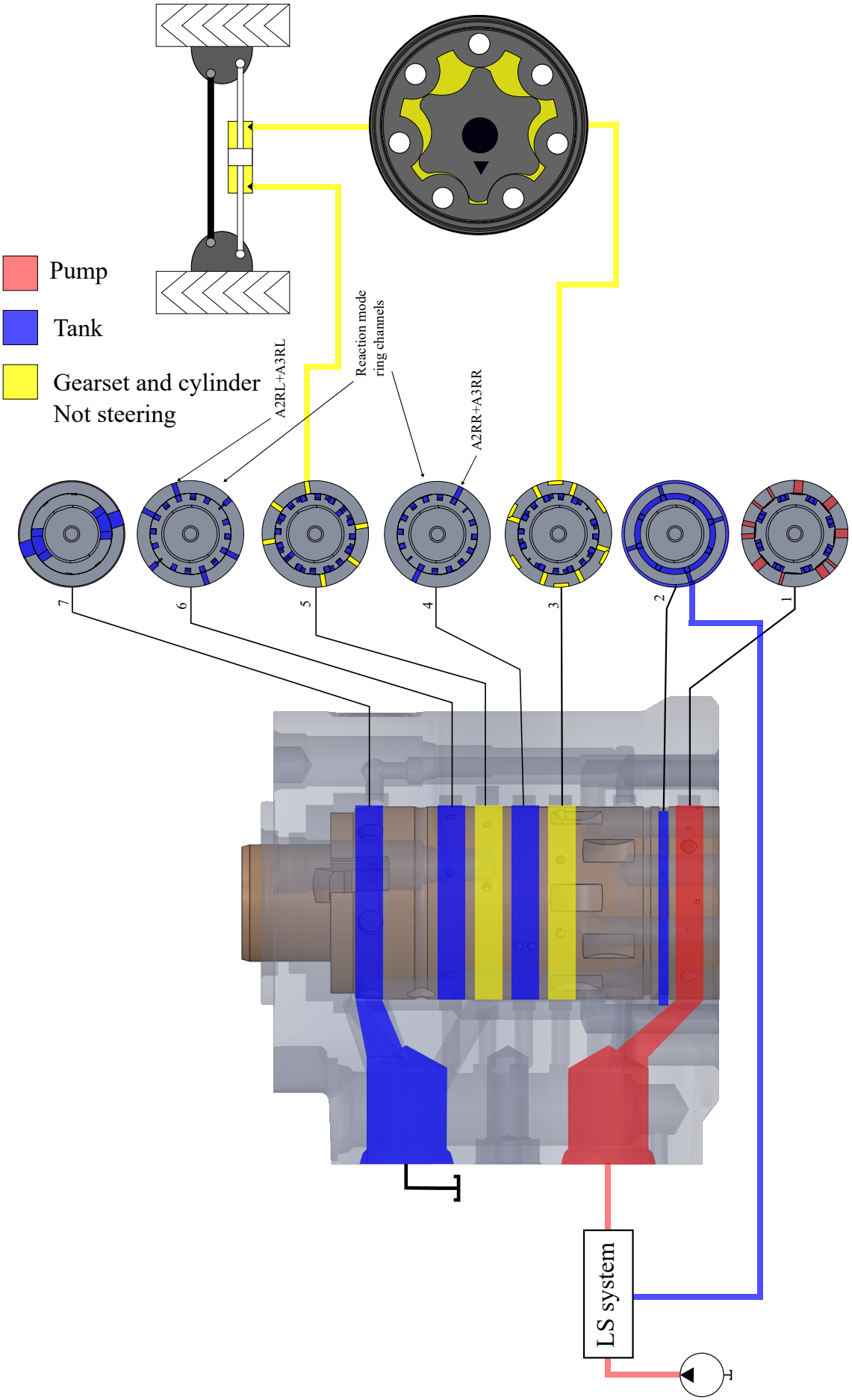

Figure 2.5. OSP system during no rotation.

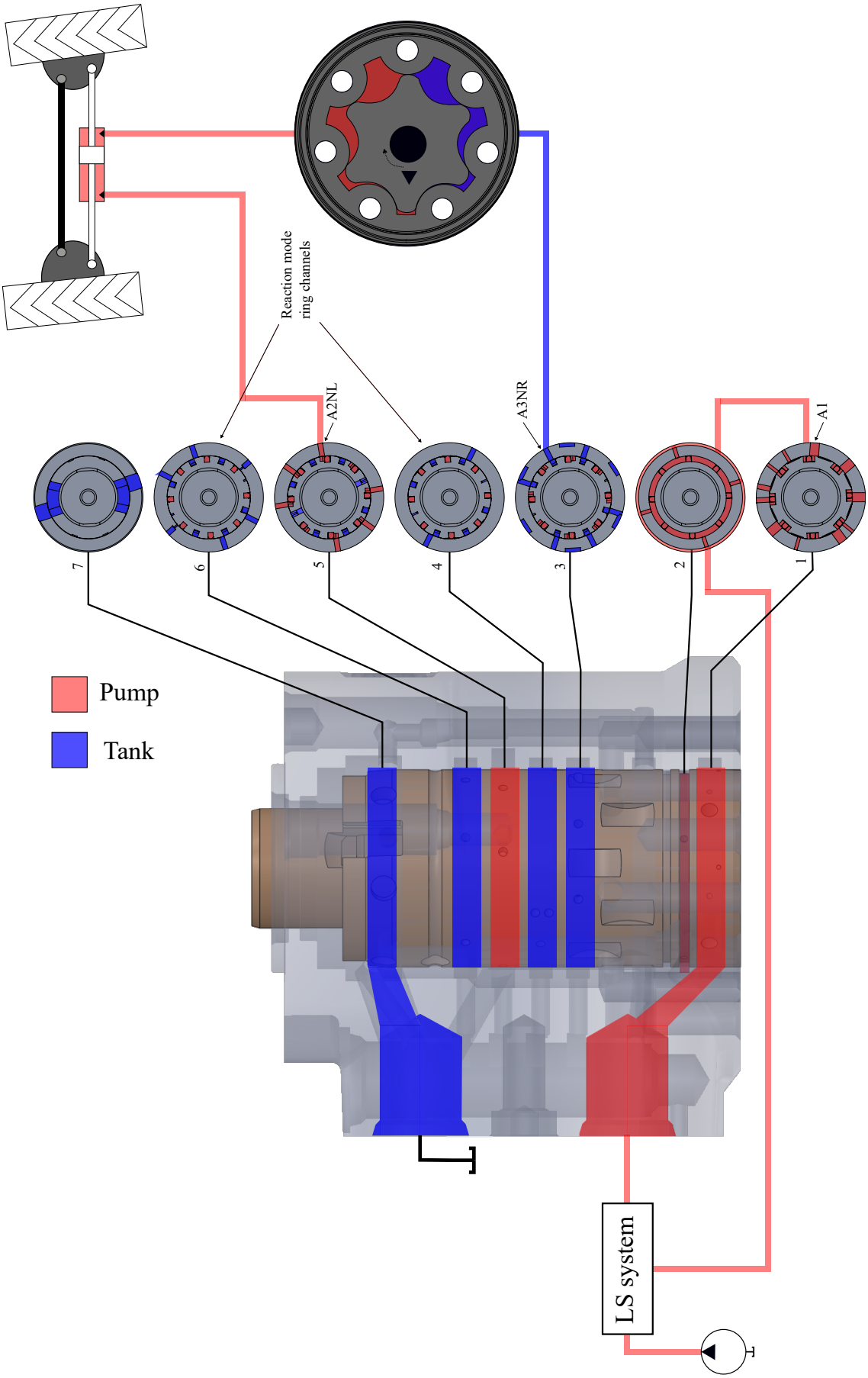

Figure 2.6. OSP system during a left rotation.

Figures 2.7 and 2.8 showcase an unfolded view of the spool and sleeve and the sleeve and house respectively.

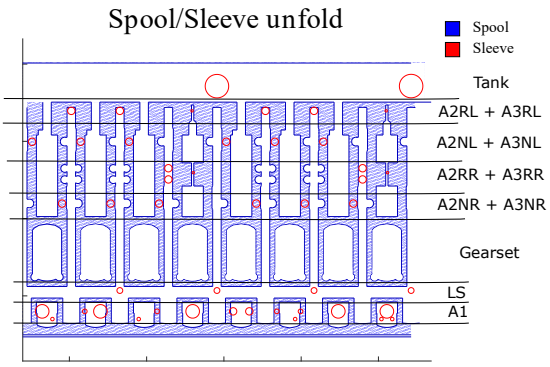

Figure 2.7. Unfolded view of spool/sleeve in neutral. Larger view in Figure A.11. [2]

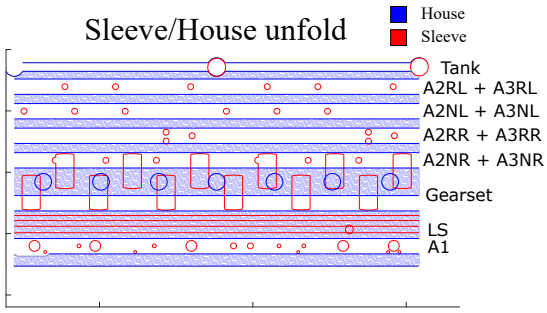

Figure 2.8. Unfolded view of sleeve/house in neutral. Larger view in Figure A.12. [2]

In these figures the holes of the sleeve can be seen on the spool and house respectively. In the spool there are several channels from "LS" to "A2RL + A3RL" these are referred to as guide channels, while in the house there are channels allowing each individual the fluid going through the sleeve holes to connect, these channels will be referred to as ring channels. These are in neutral and as can be seen the "A2RR + A3RR" and "A2RL + A3RL" are placed along the guide channel in this case. These are the reaction mode holes. This allowing fluid through during no to small rotations of the steering wheel.
Figures 2.9 and 2.10 shows the unfolded view during a turn to the left and right respectively. In Figure 2.9 it can be seen that fluid from the pump goes through "A1" from here it goes to the "LS" ring channel and then it flows along the guide channels. Here the spool and sleeve aligns such that "A2NL + A3NL" is connected to the guide channel allowing fluid to the left side of the cylinder, this will then go through the gearset as mentioned earlier. This will allow pressure build up in the left cylinder chamber and thus actuate the cylinder to the right. From here the return pressure passes through "A2NR + A3NR" and along the spool it goes to the tank. During a right turn it operates very similarly as the fluid now goes to the gearset through "A2NR + A3NR" and goes to the tank through "A2NL + A3NL". Notice that 2 areas represent the guide channels, this is because the same holes are used to function as e.g. A2NR and A3NR. The area characteristics are shown in Figure 4.1.

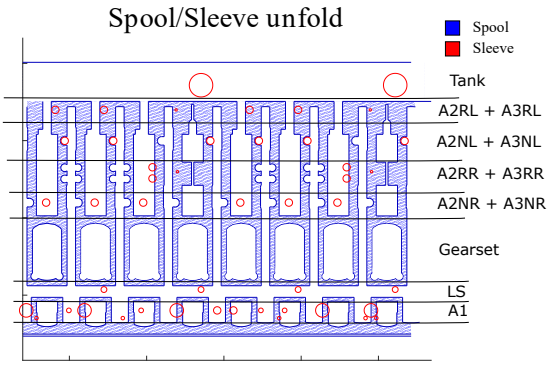

Figure 2.9. Unfolded view of spool/sleeve during left turn. Larger view in Figure A.13.[2]

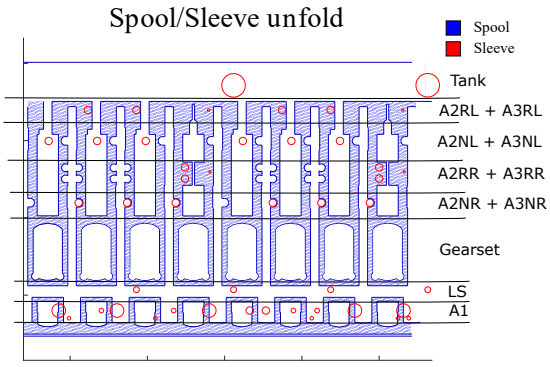

Figure 2.10. Unfolded view of spool/sleeve during righ turn. Larger view in Figure A.14.[2]

2.2 System Leakage

The OSP system allows precise operation of agricultural vehicles. However, as mentioned in the introduction leakage result in the steering wheel angle being offset after operation. This leakage occurs inside the OSP between the house, sleeve and spool. As these can rotate freely there is a margin of tolerance between the inner and outer diameters of each of the three components. The margin of tolerance results in leakage between the chambers. Between the house and sleeve there will be leakage between the ring channels, the leakage will occur from high to low pressure, during a left turn as seen in Figure 2.9. This results in a leakage from the pump side to the gearset ring channel and then to tank through the A2NR + A3NR ring channel. Furthermore, leakage will also occur between the spool and sleeve. In this case the hydraulic oil will leak from the guide channels to the tank and gearset channel. These leakages can be seen in Figure 2.11.

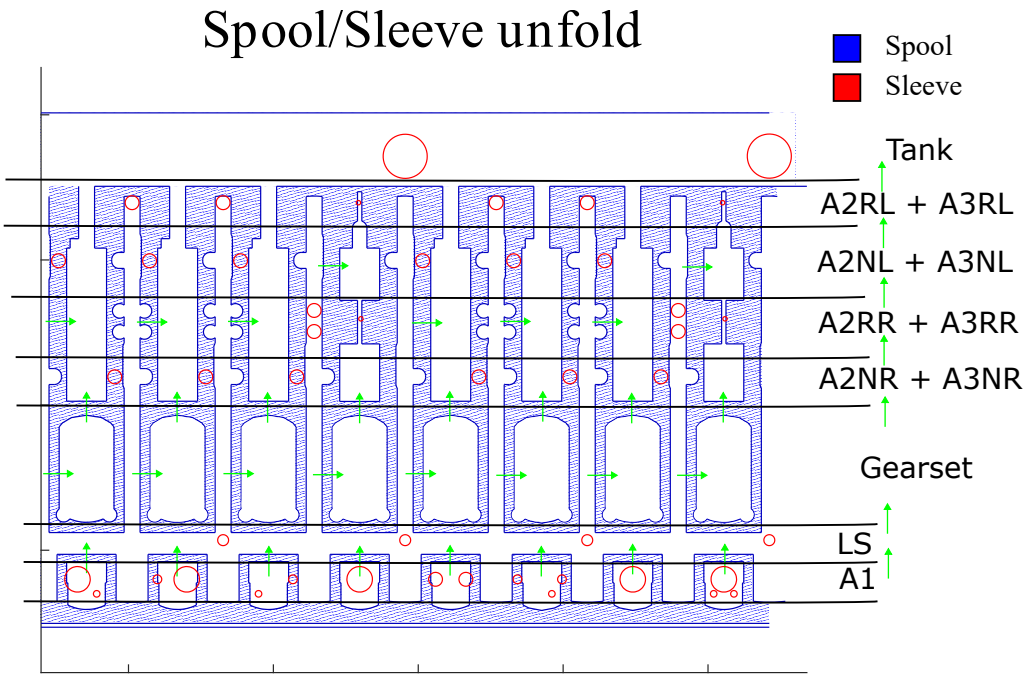

Figure 2.11. Spool and sleeve unfold in neutral. Green arrows indicate leakage ways through the tolerance between the spool and sleeve.[2]

While these leakages reduce the efficiency of the hydraulic system they will not contribute to the drift issue as the leakage in this case will be even on both sides. However, there will also be leakage in the gearset. Due to tolerance between the distributor plate and gearset as well as between the end plate and gearset, oil will leak to the middle of the gearset which is connected to the tank, as can be seen in Figure 2.2. These leakages are illustrated in the hydraulic diagram, as seen in Figure 2.12. Here there is both a leakage from the cylinder side of the gearset (Q_{leak1}) and from the side either going to tank or allowing fluid from the pump (Q_{leak2}).

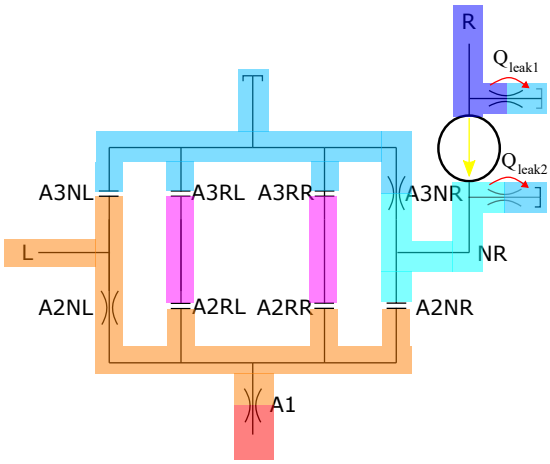

Figure 2.12. Hydraulic system during left rotation, red arrows display leakage from the gearset to tank, the yellow arrow display leakage through the gearset

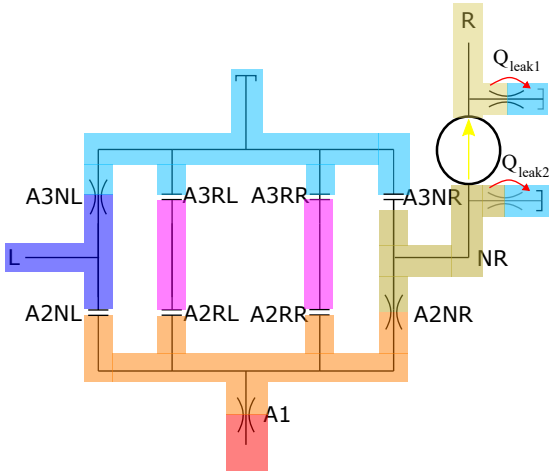

Figure 2.13. Hydraulic system during right rotation, red arrows display leakage from the gearset to tank, the yellow arrow display leakage through the gearset

Due to the gearsets placement on the right side of the hydraulic system, the leakage will be uneven. This is due to the pressure difference between the NR and tank as well as between R and tank will be higher during a clockwise rotation where it is the pressurised side of the cylinder rater than during a counter-clockwise rotation where this side is used as the return side of the hydraulic system. This is illustrated in Figures 2.12 and 2.13 where the blue color shades represent lower pressures while the red color shades represent higher pressure. Furthermore, it is possible that the tolerance between the gearset and the plates causing the leakage path can differ depending on steering direction, as the tolerance is known to be in the scale of micro meters rotation of the components can adjust how the tolerance is spread between the 2 leakage ways, which can result in significant increases to the leakage as will be discussed in Section 4.2.4 and shown in Figure 4.5.
There will also be a leakage between the NR and R side due to the tolerance resulting in a leak through the gearset. However, this leakage should only result in the gearset displacing oil at a greater rate than anticipated. While this leakage affects how the system works it should not be a benefactor to the drift issue as the oil in this case remains in the hydraulic system.
To further examine the leakage in the gearset the report will implement the leakage in the model of the OSP hydraulic system from [1].

Problem Statement 3

In the problem analysis, it was found that leakage through the gearset in the OSP is uneven, meaning during a right rotation the leakage will be larger than during a left rotation. This was determined to be the fault resulting in the steering wheel not returning to its neutral position after operating a vehicle with an OSP unit. Based on this the purpose of the report is to examine the following:

How can the leakage in the gearset of the OSP be modelled, and how can this model be used to analyse ways to reduce the drift?

Modelling 4

This Chapter will explain the modelling process of the OSP unit. This will include the [1] model as well as the additions made to it in this report. These additions being an elaboration on the gearset leakage as well as the implementation of reaction mode in the model. Due to some of this model already being part of another project the hydraulic model from [1] is in Appendix A.1. This chapter will heavily reference to this Appendix.

4.1 Spool and Sleeve Mass-Spring-Damper

The hydraulic system is operated through a Mass-spring-damper (MSD) system. Here the model input will be the steering angle θ_{ST}. This is mechanically connected directly to the spool of the OSP seen in Figure 2.2. Meaning that the steering wheel angle is equal to the angle of the spool:

$$\theta_{ST} = \theta_{SP} \tag{4.1}$$

When the steering wheel is turned the spool will turn with it. Between the spool and sleeve there is a spring, due to this the sleeve will follow the spool as can be seen in Figures A.1 and A.2. This angular deflection between the spool and sleeve will be referred to as φ, with positive direction being defined as when the spool leads the sleeve in clockwise rotation, this is illustrated in Figure A.1.
This part of the model is the same as in [1] for the modelling equations refer to Equations (A.1) to (A.7).
An addition to this model is reaction mode. This includes some different orifice areas compared to [1]. Thus the areas depending on φ in this model is given from Figure 4.1.

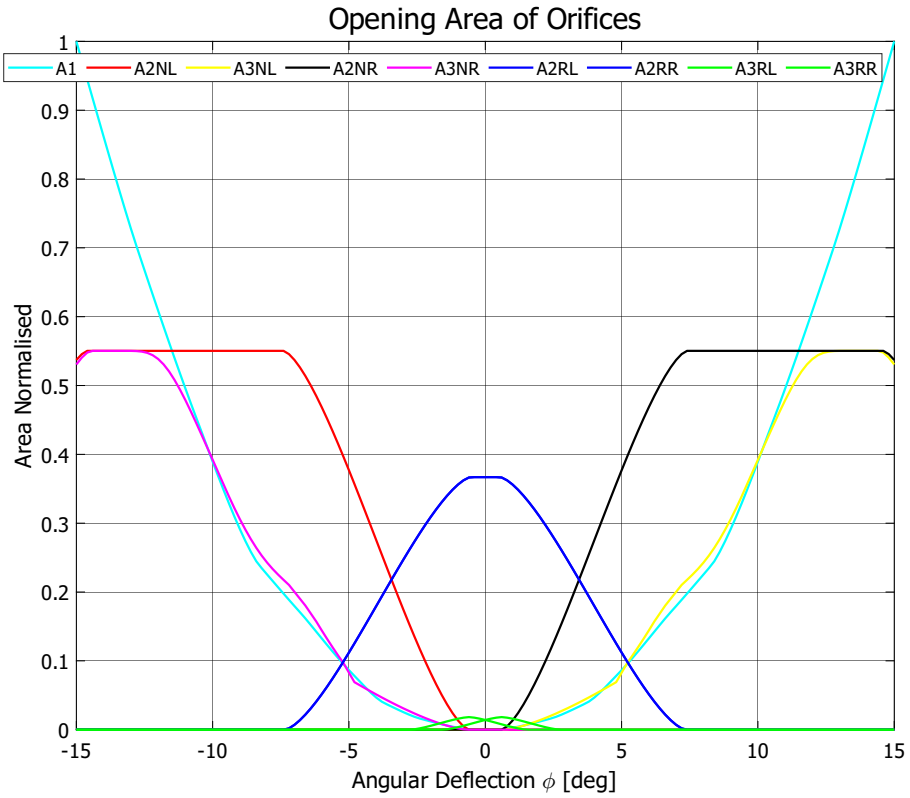

Figure 4.1. Areas as a function of φ.[2]

4.2 Hydraulic System

The hydraulic diagram for the OSP hydraulic system can be seen in Figure 4.2.

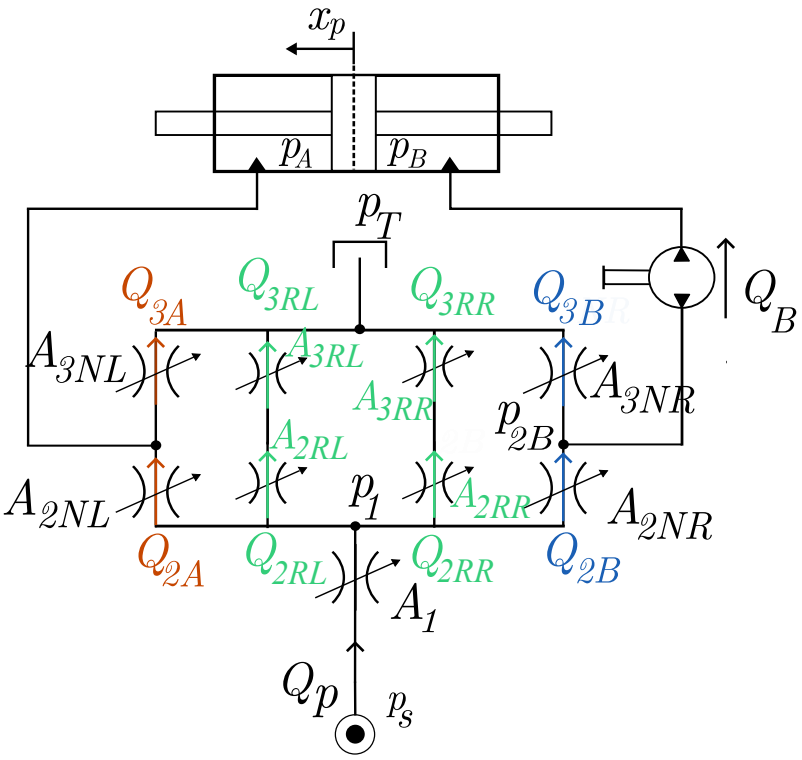

Figure 4.2. Hydraulic model from [1] with reaction mode.

As mentioned in Section 4.1 the orifice areas open depending on the angular deflection φ considering Figure 4.1 it can be seen that a clockwise rotation will result in a positive φ, thus opening A3NL and A2NR. Observing Figure 4.2 this will result in a leftward cylinder movement which also is defined as the positive direction. If φ instead is negative A2NL and A3NR will open resulting in the cylinder moving right. This fits with what has been mentioned in Section 2.1.

4.2.1 Flow Modelling

This system is modelled using the orifice equations these can be seen in Equations A.9 to A.14. It should be noted that this report has renamed some of the flows compared to [1] as mentioned in Table A.1, therefore:

$$Q_A = Q_{2A} \tag{4.2}$$

$$Q_{3NL} = Q_{3A} \tag{4.3}$$

$$Q_{3NR} = Q_{3B} \tag{4.4}$$

It is also here that the LS system is modelled in Equation (A.9), here the pressure difference is modelled such that p_p will always be 15 bar higher than p_1. In practice this is also what the LS system does, however simplifying this might suppress some dynamics of the priority valve used in the system. This is discussed further in Section 6.2.
Furthermore, the addition of the reaction mode orifices will also result in Equation (A.14) not being used in this model. Instead the reaction mode flows will be modelled as:

$$Q_{2RL} = k_v\, A_{2RL}(\varphi)\sqrt{|p_1 - p_{2L}|}sign(p_1 - p_{2L}) \tag{4.5}$$

$$Q_{3RL} = k_v\, A_{3RL}(\varphi)\sqrt{|p_{2L} - p_T|}sign(p_{2L} - p_T) \tag{4.6}$$

$$Q_{2RR} = k_v\, A_{2RR}(\varphi)\sqrt{|p_1 - p_{2R}|}sign(p_1 - p_{2R}) \tag{4.7}$$

$$Q_{3RR} = k_v\, A_{3RR}(\varphi)\sqrt{|p_{2R} - p_T|}sign(p_{2R} - p_T) \tag{4.8}$$

With p_{2L} being the pressure between the A2RL and A3RL orifices, and p_{2R} being the pressure between the A2RR and A3RR orifices.
Due to the gearset the Q_B flow is not given as an orifice equation, but will instead be given as:

$$Q_B = D_{\dot{\theta}_{SL}}\dot{\theta}_{SL} + C_{Le1}(p_{2B} - p_B) \tag{4.9}$$

This differs from [1] as the leakage going to the tank, which is the focus of this report, was modelled in a rough simplification which can be seen in Equation (A.15). In this report the leakage will be modelled differently and it is therefore not included here. The leakage that remains here is a leakage going through the gearset from p_B to p_{2B} this is visualised in Figure A.7.

4.2.2 Pressure Modelling

The pressures in the hydraulic system are modelled using the continuity equations. This can be seen in Equations (A.17), (A.18), (A.20) and (A.21) However, due to the modelling of the gearset leakage Equations (A.18) and (A.21) are adjusted to Equations (4.12) and (4.13). This will be further explained in Section 4.2.4

4.2.3 Cylinder Forces

The cylinder force is modelled using Newtons 2. Law. The equations are the same as in [1] and can be seen in Equations A.22 to A.25. Furthermore, Equation (A.25) mentions the tire forces affecting the cylinder. The steering geometry and tires have been modelled in [1], these will not be discussed here or further elaborated on but serves as a dynamic load on the cylinder in the model.

4.2.4 Modelling of Leakages

The leakages discussed in Section 2.1 will be implemented in a model made in an earlier project [1]. As mentioned in Section 2.1 the leakage going through the gearset will be the main benefactor of the drift as the leakage will be larger when steering to the right. In this case the leakage is the flow going from the gearset to the tank through the tolerances between the gearset and the distributor-plate and end-plate. Flow between parallel plates is laminar as mentioned in [4]. Thus the leakage of each gap is given by the flow found in Equation (4.10).

$$Q = \frac{\delta \, \pi \, D}{12 \, \mu \, L} \Delta p \tag{4.10}$$

With D being the diameter of the hole going to the tank which the oil is leaking to, δ being the tolerance between the gearset and the plate, and L being the length the leakage path. This is illustrated in Figures 4.3 and 4.4.

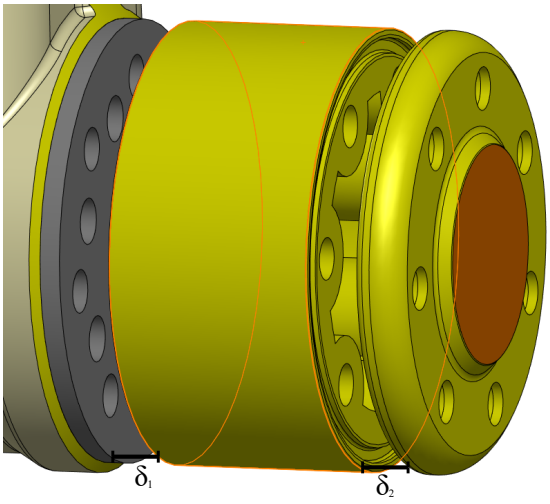

Figure 4.3. δ in the physical system.[2]

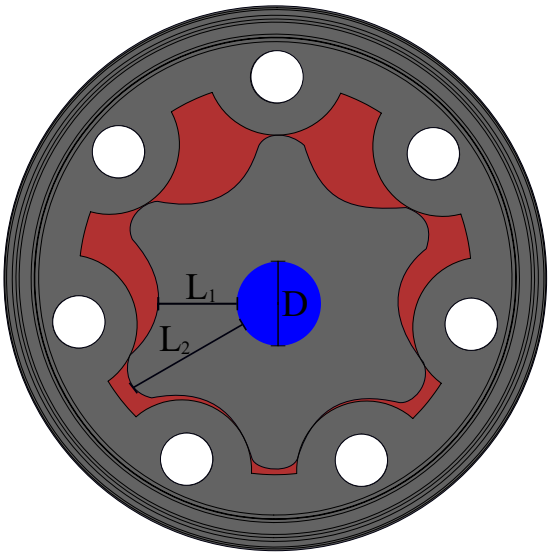

Figure 4.4. D and L of the physical system

The diameter of the hole going to the tank is known and constant, similarly the lenth of the leakage gap is determined by the size of the gearset as the oil travels past it. The teeth of the gear result in the length of the leakage path to differ. To give an estimate of the averege lenght L is given as:

$$L = \frac{L_1 + L_2}{2} \tag{4.11}$$

With L_1 and L_2 given as seen on Figure 4.4.

It should be noted that in the OSP gearset there will be 2 leakages from the gear to the tank as the oil can both go along the gap between the gear and the distributor-plate as well as the gap between the gear and the end-plate, as seen in Figure 4.3.
These leakages are added to the continuity equation for p_B and p_2B. Adding the leakages result Equations (4.12) and (4.13) respectively:

$$\dot{p}_B = \frac{\beta_{eff}}{V_{DB} + A_B \frac{x_{max}}{2} + A_B\, x_p} \left(Q_B - \dot{x}_p A_B - Q_{leak.B}\right) \tag{4.12}$$

$$\dot{p}_{2B} = \frac{\beta_{eff}}{V_{2B}} \left(Q_{2B} - Q_{3B} - Q_B - Q_{leak.2B}\right) \tag{4.13}$$

With

$$Q_{leak.2B} = \left(\frac{(\delta_1 + \delta_2)\,\pi\, D}{12\,\mu\, L}\right) (p_{2B} - p_T) \tag{4.14}$$

$$Q_{leak.B} = \left(\frac{(\delta_1 + \delta_2)\,\pi\, D}{12\,\mu\, L}\right) (p_B - p_T) \tag{4.15}$$

However, the tolerance between the plates and gearset (δ_1 and δ_2) are known to vary from $15\mu m$ to $32\mu m$. This variation happens during operation, as well as the tolerance not necessarily being the same for both of the gaps. Figure 4.5 visualises how the leakage varies at different tolerances, as well as how much the leakage can vary depending on how the tolerance is distributed across the 2 gaps.

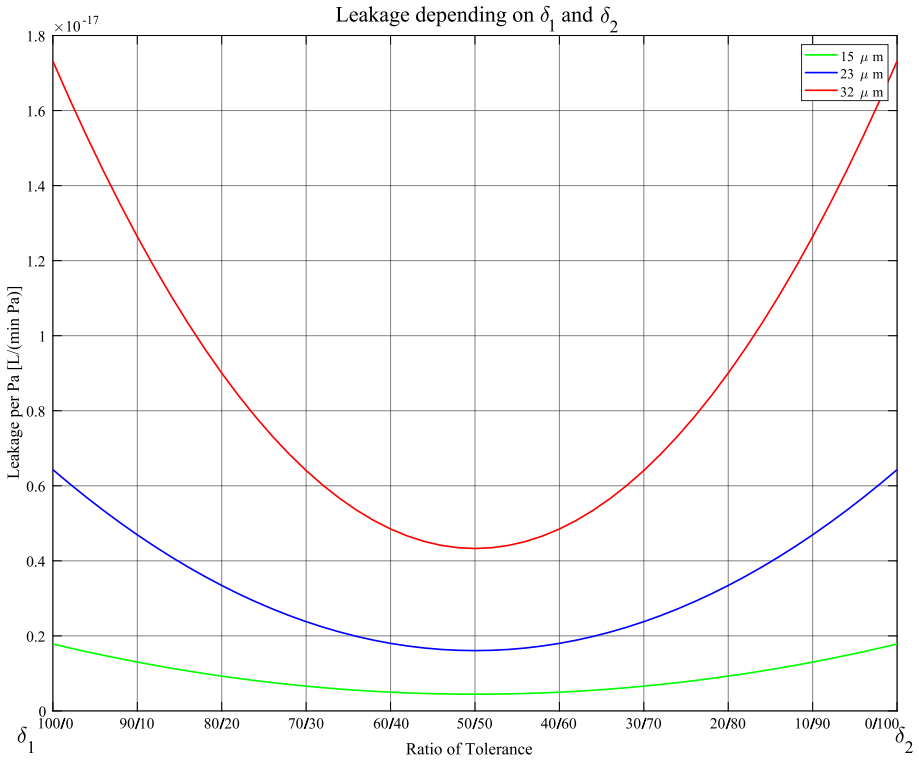

Figure 4.5. Leakage depending on the tolerances and gap height sum.

From Figure 4.5 it can be seen that there can be variations in the leakage by a factor of up to approximately 16 relative to the lowest values.

Modelling Results 5

5.1 Testing Method

The model has been tested in 3 different cases, based on experimental data recieved from Danfoss' physical testing setup. From this data the steering wheel angle is given to the model which then simulates the pressures and cylinder position.
The 3 cases at which the physical testing setup is operated consists of:

- Snake test, in this case the tractor is driven in a sinewave like manner.
- Clockwise (CW) test, here the tractor is driven clockwise around an oval.
- Counter-clockwise (CCW) test, in which the tractor is driven around the same oval but counter-clockwise

To see the effect of the leakage in the gearset tests in which the gearset leakage is excluded will also be compared to those with included leakage. As mentioned in Section 4.2.4 the leakage can vary, therefore both a scenario with a highest possible leakage as well as the lowest possible leakage are considered. These leakages are determined from Figure 4.5.
In these tests turning the steering wheel clockwise is considered the positive direction. Clockwise rotation results in the cylinder moving leftward, therefore a leftward cylinder movement (x_p) is considered to be the positive direction.

5.1.1 Snake Test

Figure 5.1 shows the snake test without the gearset leakage. Looking at the pressure difference it can be seen that the simulated response seems to fit well in the beginning, however, as the test progresses the p_B pressure becomes continuously higher than the p_A pressure. This phenomenon can also be seen to affect the cylinder position as x_p stops becoming negative, meaning the tractor does not actually turn counter-clockwise when it should.

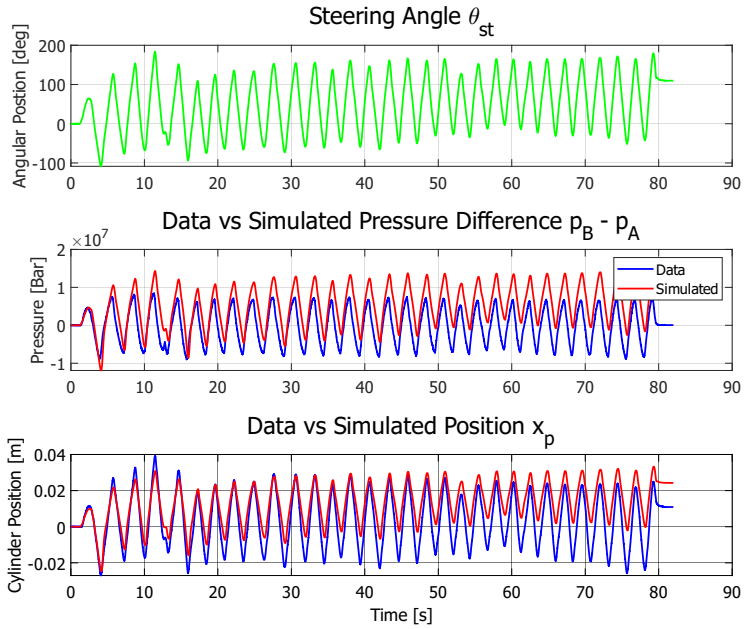

Figure 5.1. Snake test without gearset leakage

In Figure 5.2 the gearset leakage has been added, this test seems to fit significantly better, as the cylinder position (x_p) especially follows the experimental data very nicely. However, there still seems to be some issues with the pressure difference in the cylinder as throughout most of the test the pressure difference is too high.

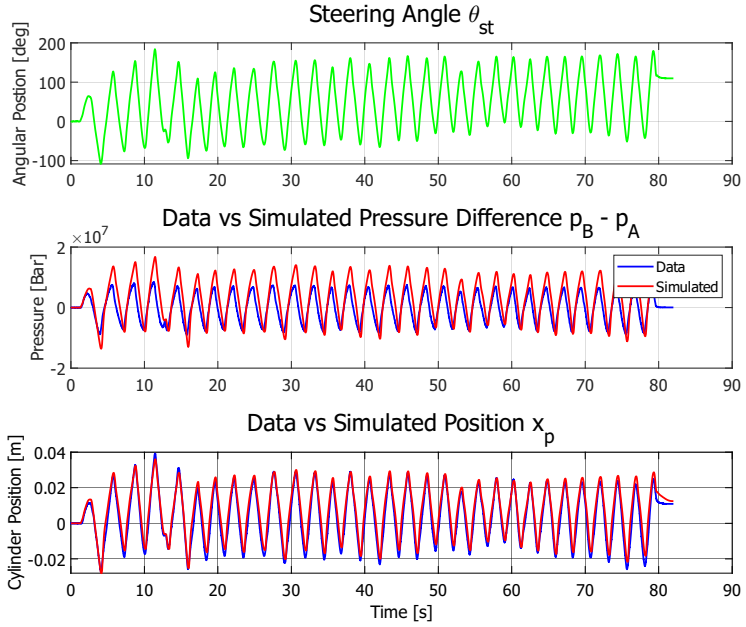

Figure 5.2. Snake test with minimum gearset leakage

Figure 5.3 has many of the same tendencies seen in Figure 5.2. However, it can be seen that the increase in gearset leakage has resulted in a slightly worse fit for the cylinder position. This increase in leakage has also affected the pressure difference in the cylinder as the leakage decreases the pressure in the p_B cylinder chamber.

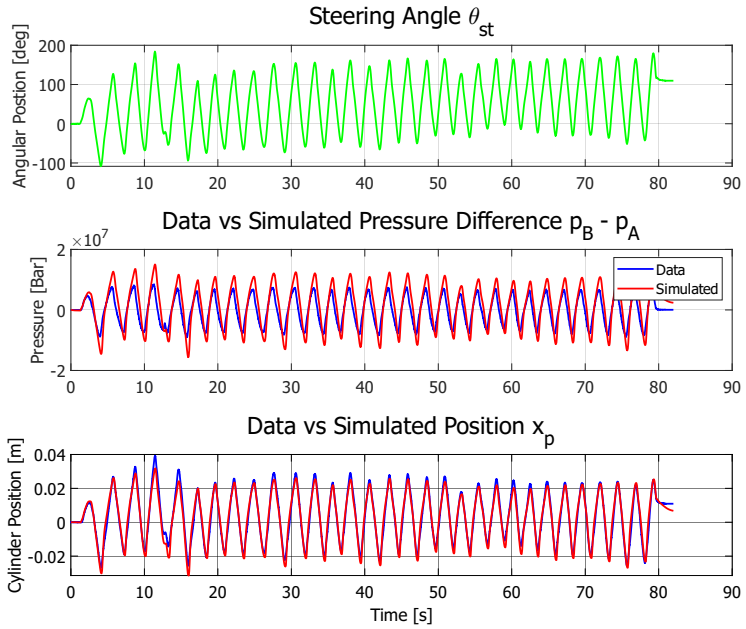

Figure 5.3. Snake test with maximum gearset leakage

The tests with leakage (Figures 5.2 and 5.3) seem to fit the experimental data quite well, as the inaccuracy in the pressure difference could be contributed to forces on the cylinder not being correct. As mentioned in [1] one of the limitations of the model is the tire model being a modelled as a simple MSD system while tires in reality are very complex. However, while this could explain the difference in pressure the main issue is the inaccuracy of the test without leakage (Figure 5.1). Due to the nature of the LS system it should be possible to track the cylinder position correctly, as the LS system in theory should increase the pressure until the desired cylinder position is increased. This is not the case in the test without leakage.

5.1.2 Clockwise Test

Figure 5.4 shows the clockwise test without leakage. In this test both the pressure difference curve as well as the cylinder position curve seem to fit. There is some offset at low cylinder movement, which result in the cylinder not reaching neutral position when it is expected to, which can also be seen in the pressure difference chart. Here the experimental data reaches 0 bar, however, this is not the case for the simulated curve.

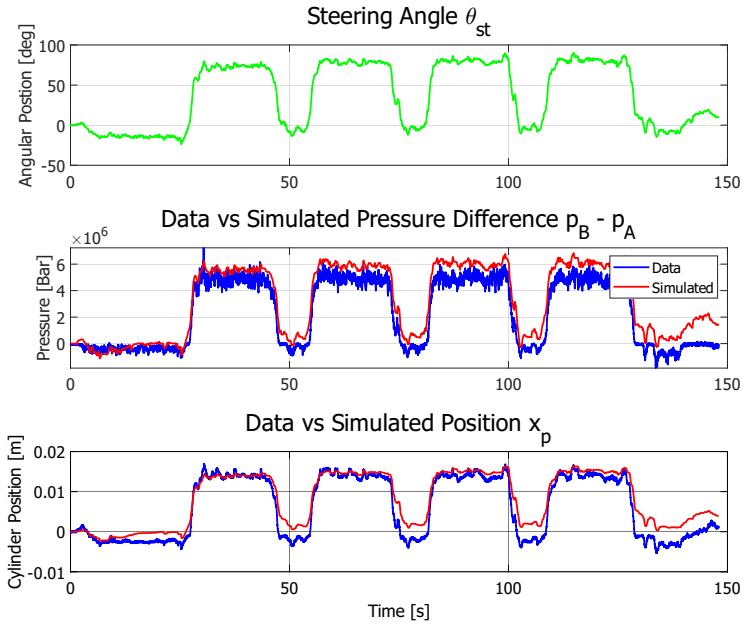

Figure 5.4. Clockwise test without gearset leakage

In Figure 5.5 the gearset leakages have been added, these seem to cause large offsets in both the cylinder position and pressure difference chart. It seems that adding the leakage causes the pressure difference to "drift" as can be seen with the pressure slowly falling in the simulated curve, while the experimental data remains a somewhat constant pressure difference level. Furthermore, the curve also "overshoots" massively while going to neutral resulting in the p_A becoming larger than p_B which causes the cylinder to not only reach neutral but also become negative. In a real scenario this means when the experimental setup stops going clockwise instead of it driving straight forward as expected from the experimental data, the model simulation causes a turn in counter clockwise direction.

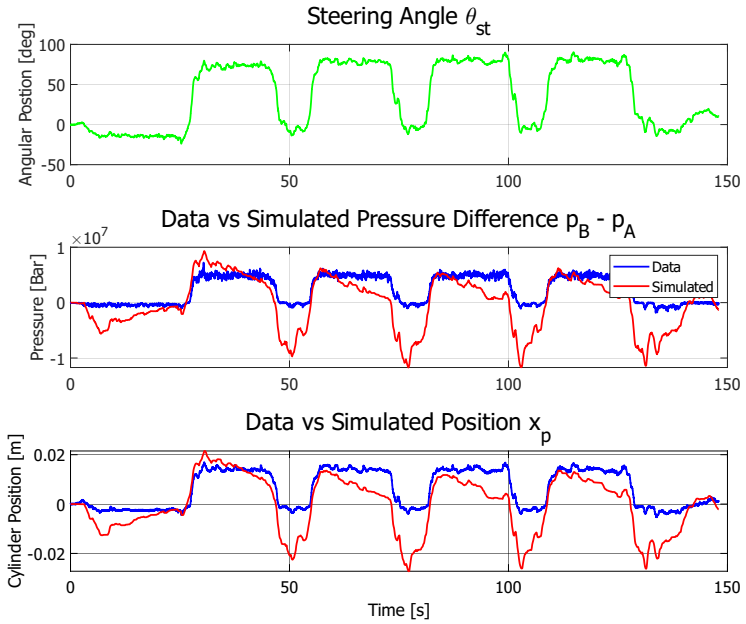

Figure 5.5. Clockwise test with minimum gearset leakage

Figure 5.6 shows very similar tendencies to the Figure 5.5, however here the persisting

drift issue is even more aggressive.

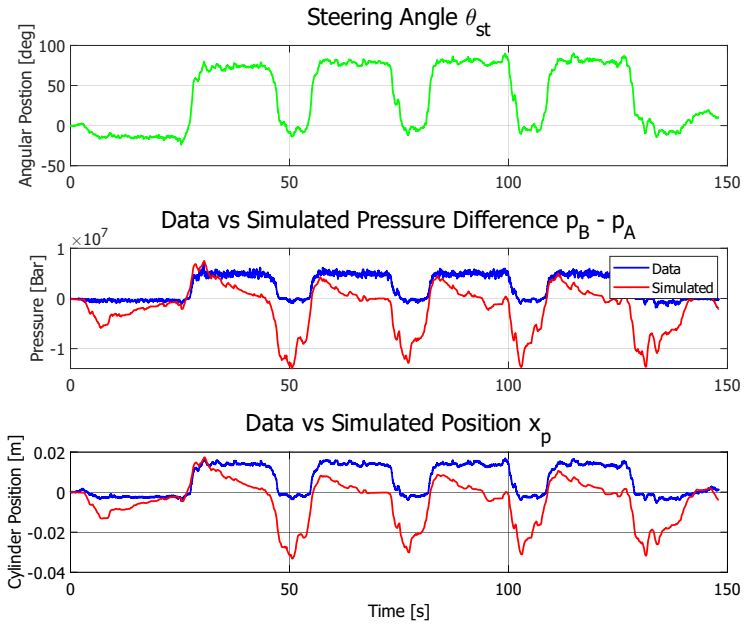

Figure 5.6. Clockwise test with maximum gearset leakage

While Figure 5.4 seemed to work as intended, the addition of the gearset leakages causes major issues in the simulated response. This confirms the conclusion in Section 5.1.1 that there are some issues with the model that cannot be explained by forces on the cylinder being incorrect.

5.1.3 Counter-clockwise Test

In Figure 5.7 the simulated response shows a tendency to drift, similarly to what was experienced in Section 5.1.2. However, while the test without leakage seemed to fit nicely in the clockwise test, this is not the case for the counter clockwise test. Here there agains seems to be a drift, this drift results in the pressure difference increasing such that the difference $p_B - p_A$ becomes much higher than expected. This in turn results in the cylinder not being able to operate in the right side of the cylinder. Something else to notice is that it seems that after the pressure difference has drifted towards neutral it stops drifting and then seems to emulate the experimental data but with an offset.

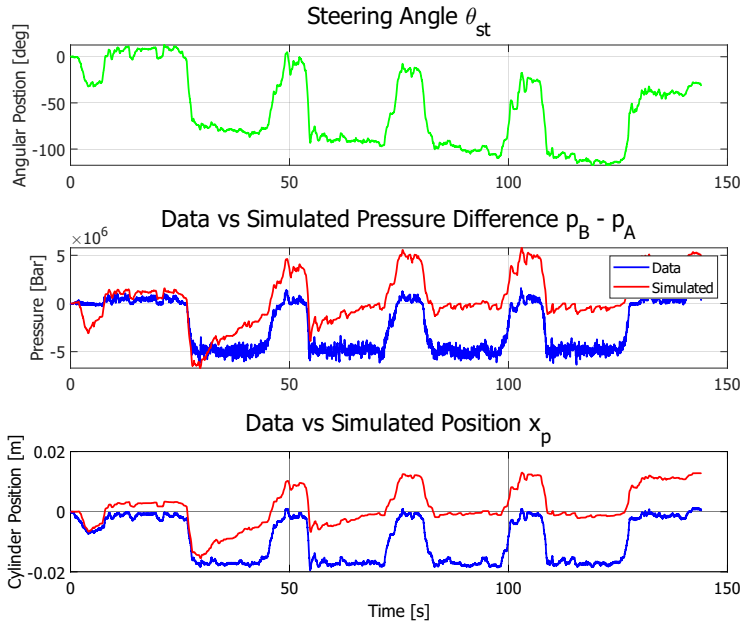

Figure 5.7. Counter-clockwise test without gearset leakage

Figure 5.8 seem to have a better fit than Figure 5.7. Here the drift towards the left side of the cylinder is reduced. However, many of the same issues still persist as seen in earlier tests. The pressure difference is too much causing the cylinder position to overshoot in both directions. As the test progresses a similar tendency as seen in Figure 5.7 is occuring as the cylinder position is slowly moving towards the left side of the cylinder causing the model to not be able to move towards the right side of the cylinder.

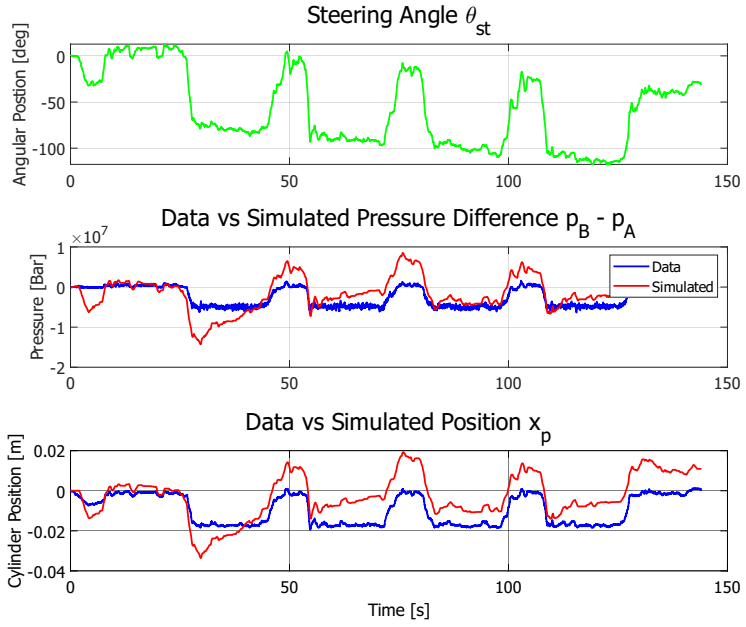

Figure 5.8. Counter-clockwise test with minimum gearset leakage

Figure 5.9 seems very similar to Figure 5.8. Here however the increase in leakage seems to reduce the issue of the cylinder position drifting towards the left side of the cylinder.

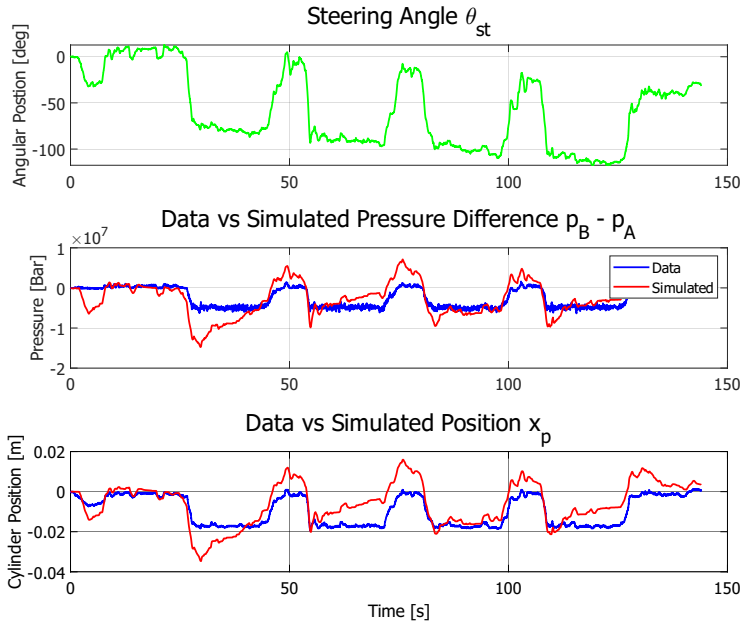

Figure 5.9. Counter-clockwise test with maximum gearset leakage

5.2 Result Conclusion

Overall there are some issues with the results. While some test seem to fit well with the experimental data others under the same conditions have issues. Generally the simulated response from the model follows the experimental data, e.g. during a clockwise turn it can be seen that the model attempts to steer the cylinder in a similar manner. However, these results also show that there are some inaccuracies in the model which causes it to drift and work in ways which are not intended. Therefore the model will be further analysed.

Result Analysis 6

6.1 Pressure Analysis

To further analyse the results from Chapter 5 the pressures will be further examined. In Chapter 5 it was found that the addition of leakage adjusted the results significantly however the size of the leakage way only seemed to amplify this change. Therefore, the analysis focuses on the test without leakage as well as the test with maximum leakage. Furthermore, the p_{2B} pressure is not available for the physical testing setup. The simulated p_{2B} pressure will be included for the analysis but cannot be compared to experimental values.

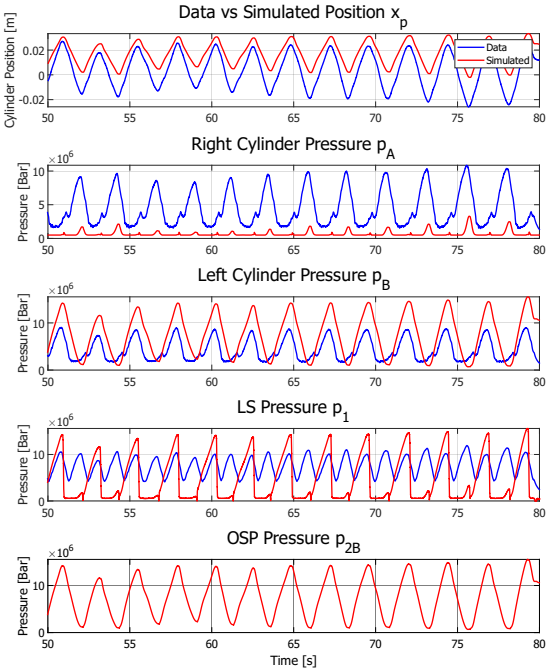

Figure 6.1. Zoomed view of pressure from snake test without leakage

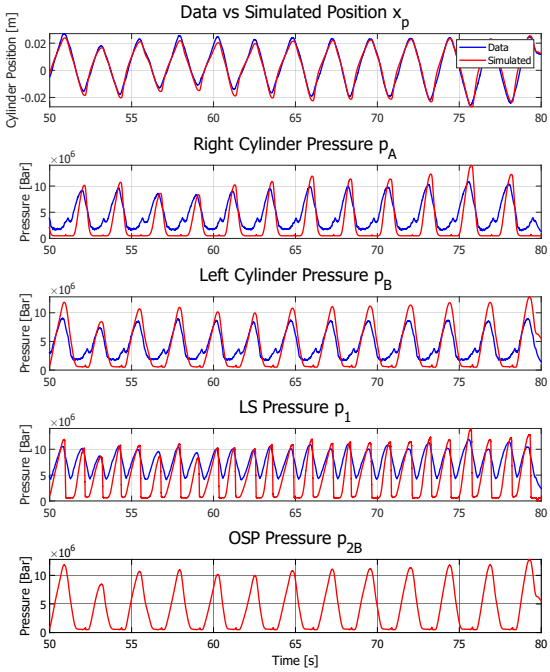

Figure 6.2. Zoomed view of pressure from snake test with leakage

From Figures 6.1 and 6.2 it can be seen that while Figure 6.2 seems to fit nicely there are some issues with the p_1 pressure as the simulated pressure seems to reach tank pressure whenever a counter-clockwise rotation of the steering wheel is made while in reality the pressure should be maintained at a higher level. However, Figure 6.1 shows even more issues with the p_1 pressure. Here it can be seen that the p_1 pressure only increases during clockwise rotations thus resulting in the cylinder position being unable to move to the right side of the cylinder. This results in p_A not being pressurised when it is supposed to and thus the tractor is unable to steer counter-clockwise as was seen in Figure 5.1.

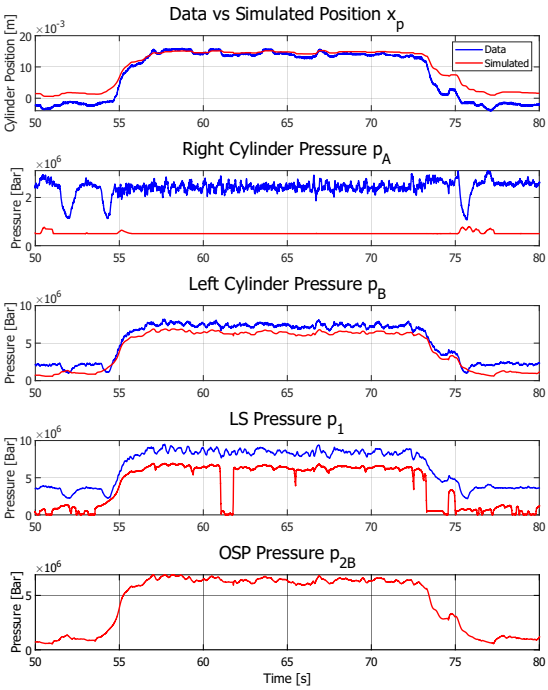

Figure 6.3. Zoomed view of pressure from clockwise test without leakage

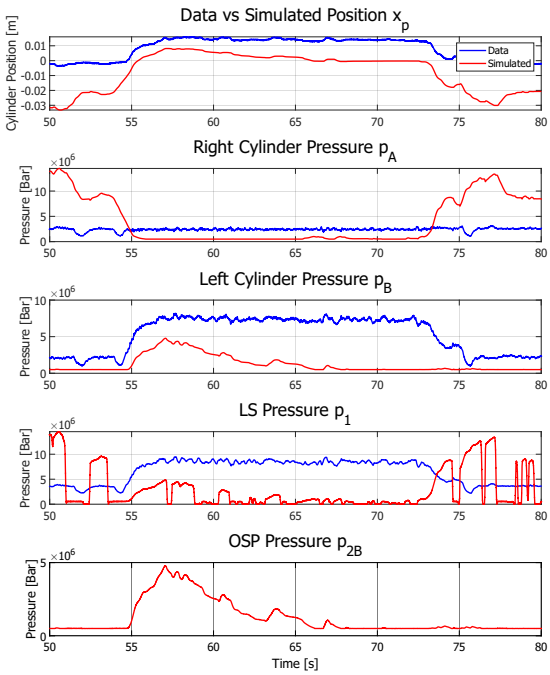

Figure 6.4. Zoomed view of pressure from clockwise test with leakage

Figures 6.3 and 6.4 shows similarities to Figures 6.1 and 6.2. While Figure 6.3 works as intended most of the time it can be seen that there are some issues with p_1. The fact that it is offset is not problematic as this could be explained by forces on the cylinder which are not accounted for. However, the sudden drop in the p_1 pressure around 61 seconds should not happen even if the cylinder position fits regardless. Furthermore, Figure 6.4 is completely off and p_1 almost seems to work opposite of what is intended as pressure is high during no steering wheel rotation and low during steering wheel rotation. It can be seen that this causes p_A to be pressurised while no pressure is needed while also making the simulation incapable of steering as much as intended. Here it can be seen that this fault in p_1 directly causes the drift seen in Figure 5.6 where p_A becomes pressurised and p_B does not get the necessary pressure to operate the cylinder as intended.

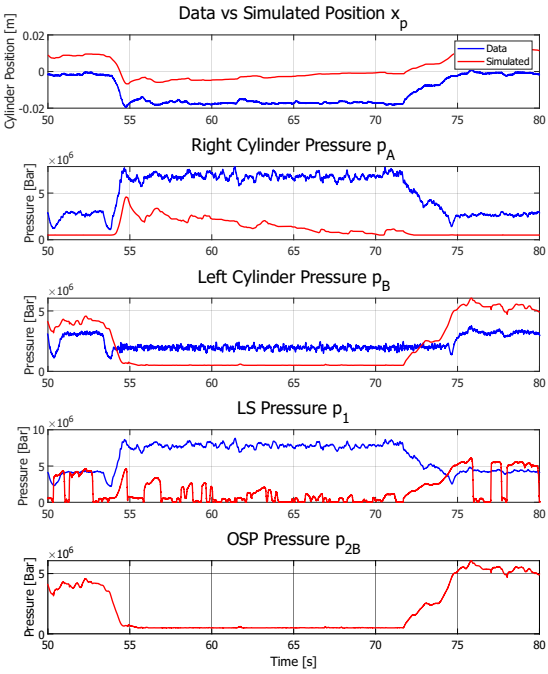

Figure 6.5. Zoomed view of pressure from counter-clockwise test without leakage

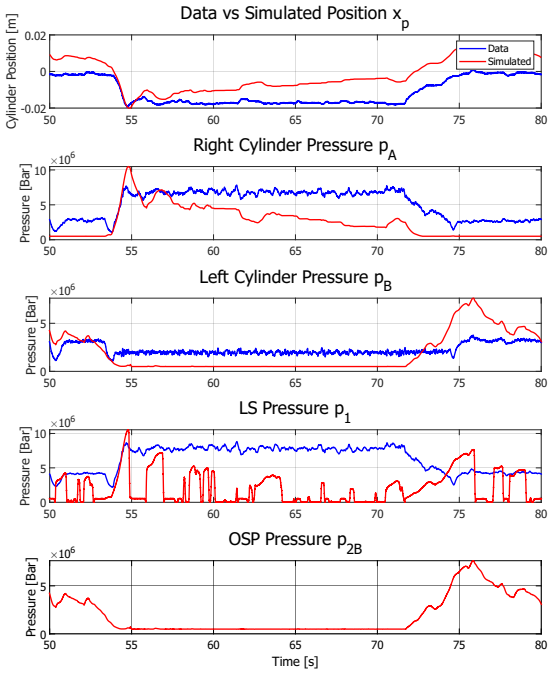

Figure 6.6. Zoomed view of pressure from counter-clockwise test with leakage

Figures 6.5 and 6.6 verifies that the p_1 issues seems to be the cause of the fault in the model. As mentioned before it seems to pressurise when it is not supposed to causing the p_B pressure to move the cylinder in the opposite direction as seen in Figure 5.7

6.2 LS Pressure Analysis

To understand why the LS pressure p_1 seems off the flow of the LS system is observed. In Figure 4.2 it can be seen that the continuity equation for p_1 is given as:

$$\dot{p}_1 = \frac{\beta_{eff}}{V_1}\left(Q_p - Q_{2A} - Q_{2B} - Q_{RL2} - Q_{RR2}\right) \tag{6.1}$$

Therefore observing the sum of the flows Q_1, which is given as Equation (6.2), should give us an idea of how this pressure is determined in the hydraulic model.

$$Q_1 = Q_p - Q_{2A} - Q_{2B} - Q_{RL2} - Q_{RR2} \tag{6.2}$$

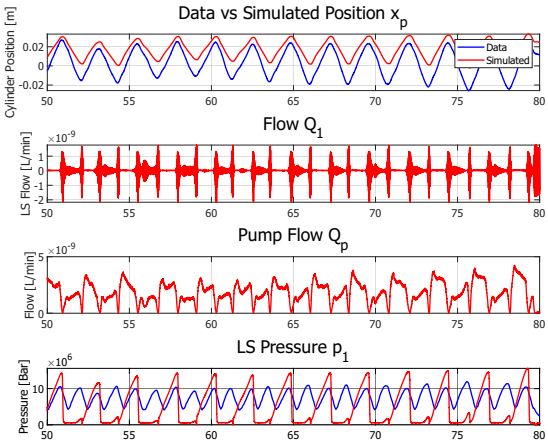

Figure 6.7. Zoomed view of snake test without leakage

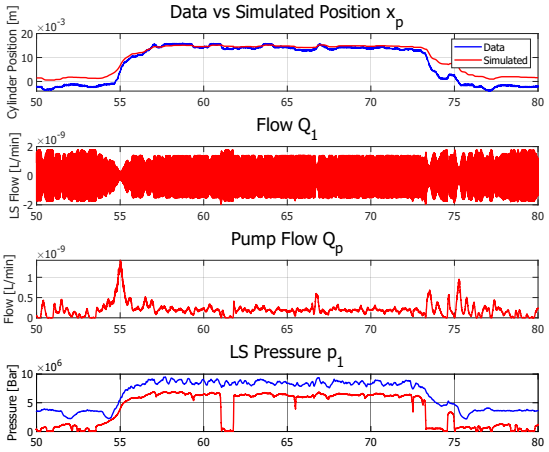

Figure 6.8. Zoomed view of clockwise test without leakage

However, as can be seen in Figures 6.7 and 6.8 the LS flow acts unexpected. These measurements are not unique and is the case for all tests shown in Chapter 5. With aall snake test having a similar Q_1 to what is seen in Figure 6.7 and for both clockwise and counter-clockwise tests Q_1 acts similarly to what is seen in Figure 6.8.
What should noted is that the LS system in the model is modelled simplistically such that the pressure difference between the pump pressure p_p and the LS pressure p_1 always is $15bar$. This should however, not cause the issues seen here.
There are many ways to make an LS system, the Danfoss OSP unit works such that the pump pressure input is compensated with a priority valve. This is done with pressure feedback from p_1 through a LS line, this LS line will then regulate the pump pressure to give enough flow to overcome the load on the cylinder. As can be seen in Figure 6.9.

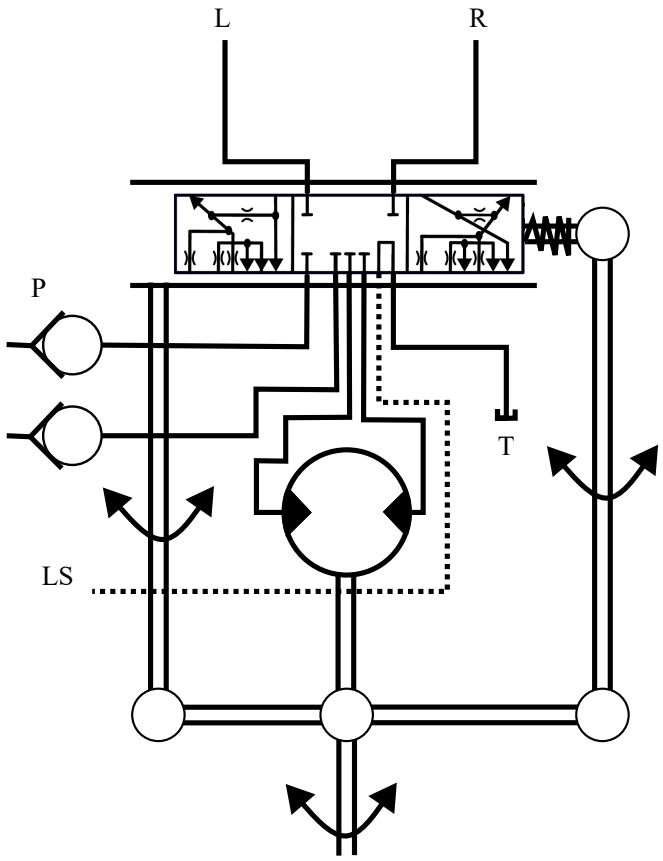

Figure 6.9. Non simplified valve schematic [3].

Therefore, while the simple model of the LS system might lack some dynamics through the response of the priority valve, this would not result in such a significant impact as is seen in the model results.
However, it can be seen in Figures 6.7 and 6.8 that the LS system increases Q_p as the steering wheel is turned and thus delivers pressure to the cylinder. This is the LS flow operating as it is supposed to. However, it seems that something goes wrong between Q_p and Q_1. T

6.3 Analysis of Spool and Sleeve Angle

To further analyse the inaccuracies seen in in Section 6.2. These flows as well as φ will be analysed. As shown in Figure 4.1 the areas opening in the OSP unit depend on the angle between the spool and sleeve of the OSP also known as φ. These tests shows the flows in the OSP during operation. For the left (Q_{2A} and Q_{3A}) and right (Q_{2B} and Q_{3B}) side flows the notation is that Q_{2B} and Q_{2A} are the pump side and that Q_{3B} and Q_{3A} are the tank side as can also be seen in Figure 4.2. The reaction mode flow is a summation of Q_{2RL} and Q_{2RR}.

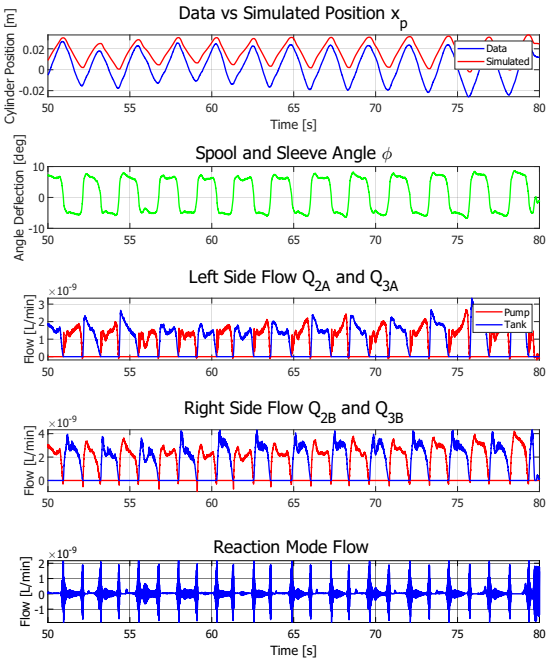

Figure 6.10. Zoomed view of flows from snake test without leakage

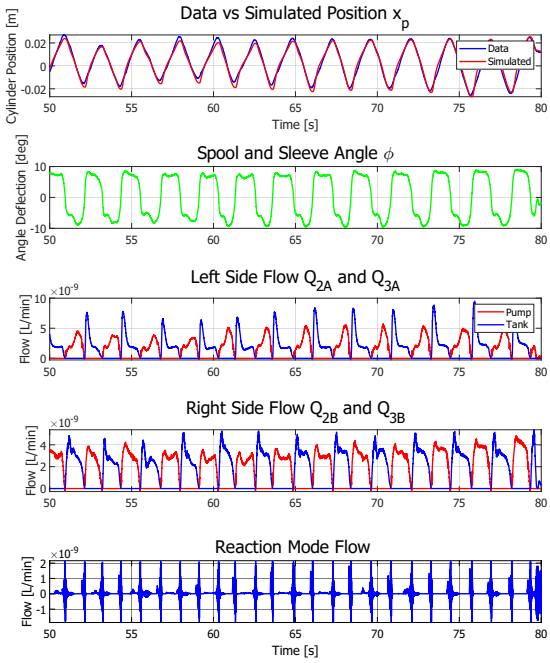

Figure 6.11. Zoomed view of flows from snake test with leakage

In Figures 6.10 and 6.11 the flows seem to function as expected it can be seen that when the steering wheel is turned clockwise there is flow through Q_{2B} and Q_{3A}. Thus resulting in the cylinder is moving to the left. Furthermore during a counter-clockwise rotation there is flow through Q_{3B} and Q_{2A} resulting in the cylinder is moving to the right. It can be seen that when φ reaches a lower angle flow is led through the reaction mode orifices as expected and as the angle increases the reaction mode orifices close again. The values of these reaction mode flows does not behave as expected, when this reaction mode flow is negative this means that the flow is going back into LS pressure p_1 rather than moving to the tank p_T through the A3RR and A3RL orifices which are also open in these scenarios. Here it would be expected that the pressure is higher in p_1 than after the reaction mode orifice, however this seems to not be the case as flow is going back into the p_1 chamber.

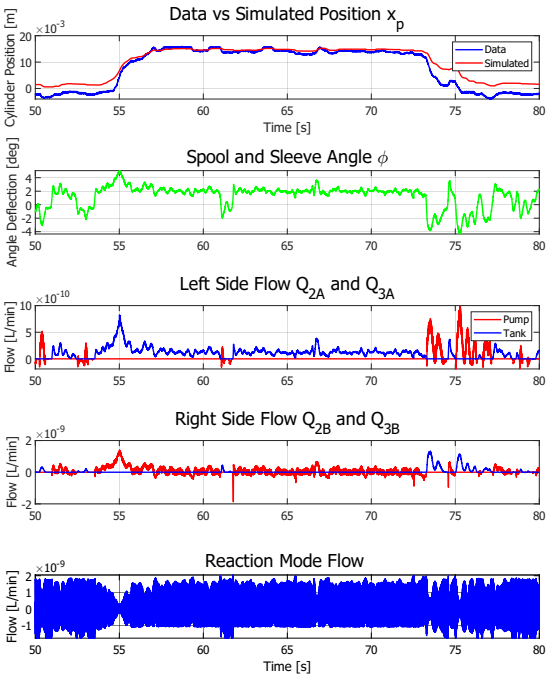

Figure 6.12. Zoomed view of flows from clockwise test without leakage

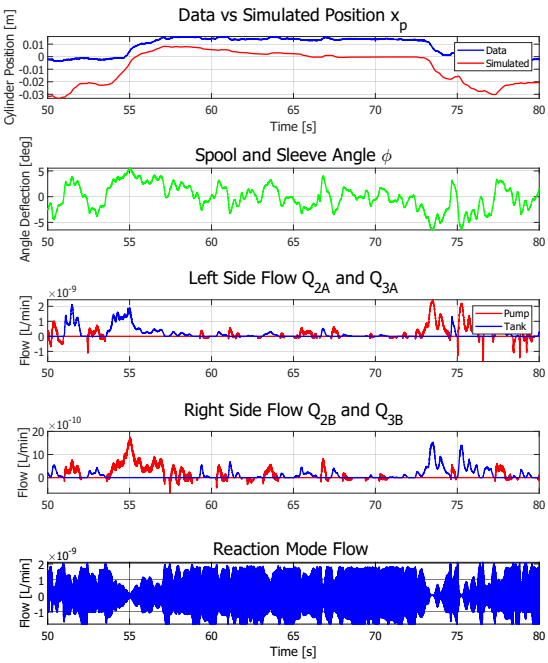

Figure 6.13. Zoomed view of flows from clockwise test with leakage

Figures 6.12 and 6.13 also seem to simulate as desired. There are some cases with Q_{2A}, Q_{3A} Q_{2B} Q_{3B} flow going the opposite way, however this is very brief and around $\varphi = 0$ where the orifices opening are meant to change. Thus this should not be a major issue. However, again the reaction mode flow fluctuates between going to p_1 and p_T in both tests. Furthermore, in Figure 6.13, φ fluctuates around 0° almost randomly. Here it would be expected that it was clear when the turn is happening and when it stops. This can be seen better in Figure 6.12 where φ goes from around 0° to 2° as the steering wheel is turned.

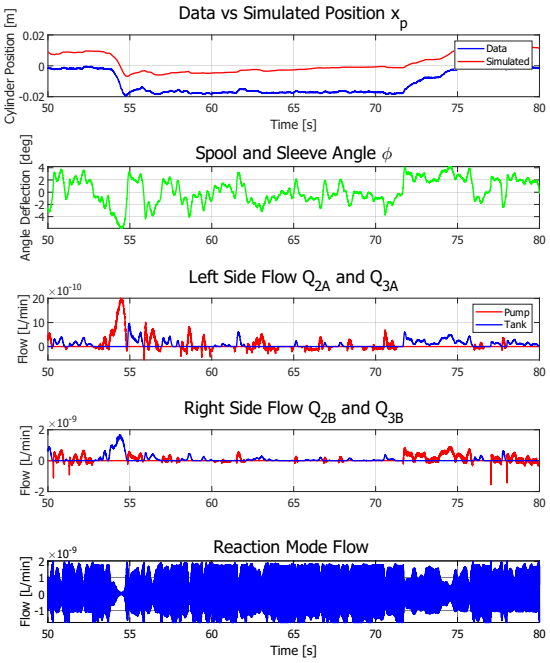

Figure 6.14. Zoomed view of flows from counter-clockwise test without leakage

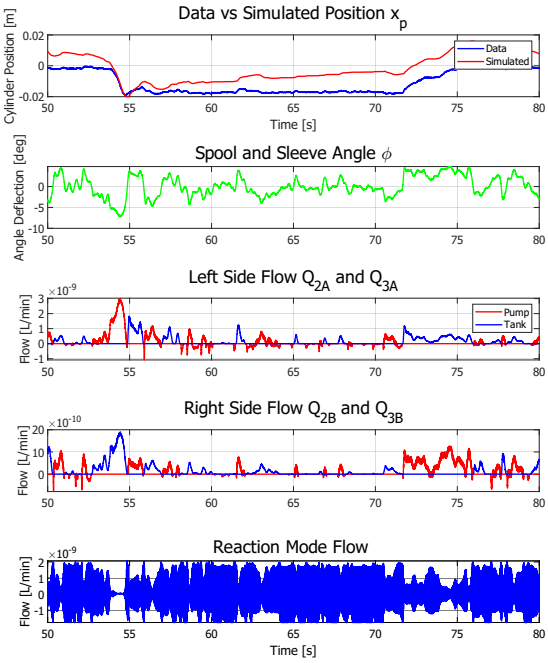

Figure 6.15. Zoomed view of flows from counter-clockwise test with leakage

Similarly to the others tests, Figures 6.14 and 6.15 has the same issues with the reaction mode flow going both ways. Furthermore, here the issue with the spool and sleeve angle fluctuating somewhat randomly, similarly to Figure 6.13, is present in both tests.

6.4 Analysis Conclusion

From these tests it seems that the issue with the cylinder position being incorrect in some tests is caused by the p_1 pressure not functioning as expected. However, based on the findings in Section 6.2 this should not be caused by the modelling of the LS pressure itself, as the simplified modelling of the LS pressure does not correlate with the errors seen in the tests. It seems from Section 6.3 that the cause of the error is either from the modelling of the reaction mode system or perhaps the spool and sleeve model as both the reaction mode flow and φ operates unexpectedly. Due to the complexity of the system it is difficult to tell what is the cause for the error in φ. As it could be caused by the mechanical system not being modelled correctly, but it is also possible that the cause is related to the hydraulic model as this affects φ as seen in Equation (A.6).

Conclusion 7

In this report the drift issue found in [1] has been further examined. Here it was found that the leakage originated from the leakage in the OSP gearset, allowing hydraulic fluid to pass through the tolerance between the OSP's moving parts. Resulting in hydraulic fluid going from p_B and p_{2B} to the tank p_T.

This report has then examined how this leakage can be modelled as well as adding danfoss' reaction mode system to the OSP model. Here it was found that the leakage in the OSP can vary by a factor of 16 depending on how wide the tolerance is and how it is placed between the 2 leakage ways.
To validate the model it was compared to 3 different experimental tests. One being the snake test in which the tractor was maneuvered in a sine wave like manner. The other 2 tests were carried out by driving the tractor around an oval track, with one test being driven around in clockwise direction and the other being driven counter-clockwise.
From these tests it was found that while some of the tests seemed to be simulated nicely, there was also some noticeable errors. In several tests there was a "drift" on the cylinder position causing it to slowly become more and more inaccurate.

Based on these test results the project further examined the pressures, flows and the mechanical spool sleeve system to locate the error. It was found that there was an issue with the LS pressure p_1 not being pressurised high enough to operate the system. It was found that this was not caused by how the LS system was modelled but rather seemed to be caused by the reaction mode flow going in the opposite direction of what was expected as well as the angle between the spool and sleeve (φ) not giving the expected response.
It was not possible to find the direct cause to these issues in the model due to the complexity of the OSP system. This is because an error in φ could be caused by the mechanical spool and sleeve system as well as the hydraulic system.

Because of this the report was not able to investigate how the drift issue experienced in [1] could be reduced.

Bibliography

[1] R. J. Sørensen and A. B. Mortensen. "Modelling and validation of a new state of the art steering system for large commercial tractors." Visited 9-2-2024. (2023), [Online]. Available: https://kbdk-aub.primo.exlibrisgroup.com/permalink/45KBDK_AUB/a7me0f/alma9921650698405762.

[2] Information given by company contact at Danfoss, Emil Nørregård Olesen.

[3] E. N. Olesen, "A case study investigation of an engineering department at danfoss with focus on the handling of digitization," Aalborg University, Tech. Rep., 2020.

[4] A. H. Hansen, *Fluid Power Systems*. Fluid Power & Mechatronic Systems Aalborg Universitet, 2019.

[5] M. N. Friis and M. A. Jensen. "Development, validation and optimization of a new steering concept." Visited 26-10-2023. (2021).

Appendix A

A.1 Model Overview

Here the model from [1] is shown for further elaboration, this is a citation. In Appendix A.1.3 there will be some comments about this citation as well as 2 figures cited from [1] that are referred to in the citation of the hydraulic model. This is included for overview of the model and is a citation of page 7-13 [1]:
“

A.1.1 *Spool and Sleeve Model*

The steering wheel controls the vehicle via the flow in and out of the hydraulic cylinder. The spool is interfacing with the spring and through the spring interfaces with the sleeve the components are seen in Figure A.1.
This angle is desired to determine the orifice area under operation and can be seen in Equation (A.1).

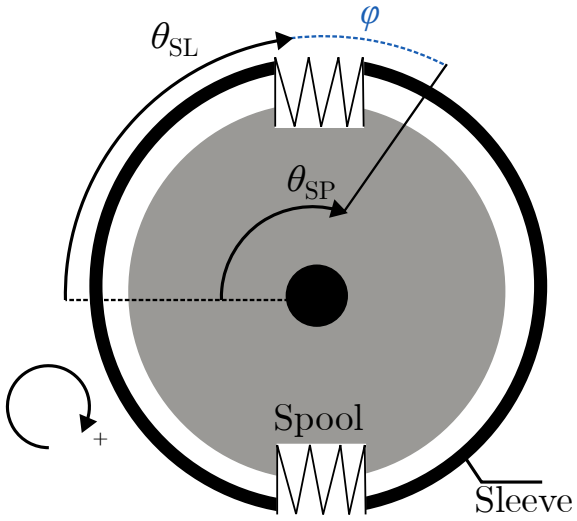

Figure A.1. *Rotation direction and torques that affect the Spool and Sleeve.*

$$\varphi = \theta_{SP} - \theta_{SL} \tag{A.1}$$

φ is the angle difference between the spool and sleeve. This angle is mechanically limited to $\pm 15°$, θ_{SP}, and θ_{SL} is the angular position of the spool and the sleeve respectively. To find this relative angle between the spool and sleeve, φ, a rotational equilibrium system is set up for both components as can be seen in the free body diagram in Figure A.2.

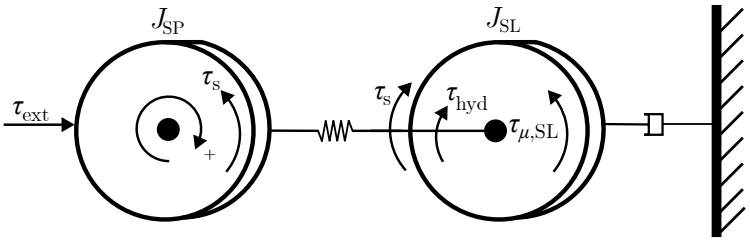

Figure A.2. *Diagram showing the forces effecting the two bodies.*

Here the interface between the spool and sleeve system is shown and the equation for the spool is derived as Equation (A.2)*.*

$$\ddot{\theta}_{SP} = \frac{1}{J_{SP}}(\tau_{ext}(t) - \tau_s(\varphi)) \tag{A.2}$$

τ_{ext} *is the external torque performed on the steering wheel by an operator,* τ_s *is the torque from the spring package, that connects the spool to the sleeve and therefore has a negative contribution to the spool and positive to the sleeve. The torque of the spring is described as Equation* (A.3)*:*

$$\tau_s(\varphi) = k(\varphi)\varphi \tag{A.3}$$

The spring constant $k(\varphi)$ *is designed to always be in compression between the spool and sleeve modeled using Equation* (A.4) *[3] [5].*

$$k(\varphi) = \frac{a\,\tanh(\varphi\, b)}{\varphi} + c\,\varphi \tag{A.4}$$

The stiffness of the spring is modeled to be varying, as a function of the deflection. Here the constants $[a, b, c]$ *in Equation* (A.4) *are fitted to the spring experimentally as seen in [5]. The relation between torque and deflection is shown in Figure A.3*

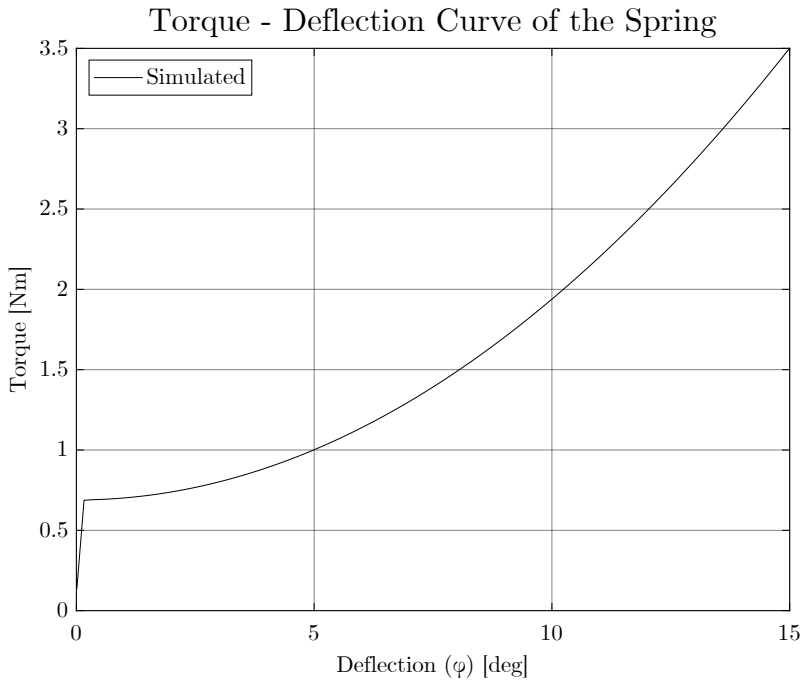

Figure A.3. *Relation between deflection of spring and torque.*

As 15° *is reached the spring will be fully compressed and the torque will be directly applied from the steering wheel to the sleeve.The Mass-Spring-Damper (MSD) system containing the sleeve is a counter torque to the spool system connected by the spring.*

$$\ddot{\theta}_{SL} = \frac{1}{J_{SL}}(\tau_{hyd} + \tau_s(\varphi) - \tau_{\mu,SL}(\dot{\theta}_{SL}) \tag{A.5}$$

Where τ_{hyd} *is the torque applied by the gear set to the sleeve through the Cardan shaft and* $\tau_{\mu,SL}(\dot{\theta}_{SL})$ *is the friction from the gear set. The torque* τ_{hyd} *is described by Equation* (A.6)*:*

$$\tau_{hyd} = D_{\dot{\theta}_{SL}}(p_{2B} - p_B) \tag{A.6}$$

Here $D_{\dot{\theta}_{SL}}$ *is the pump displacement created by the gear set. As mentioned in [5] and [3] the friction in pump units larger than 100 cc demands a more complex friction model. This entails the use of both viscous and coulomb friction as seen in Equation* (A.7)*:*

$$\tau_{\mu,SL}(\dot{\theta}_{SL}) = sign\,\dot{\theta}_{SL}\,C_{SL} + B_{SL}\,\dot{\theta}_{SL} \tag{A.7}$$

Here B_{SL} *is the viscous friction constant and* C_{SL} *is the Coulomb friction constant. These are fitted according to [3] and [5].*

A.1.2 *Hydraulic Section*

In this section, a lump parameter hydraulic model will be made to be consistent with Figure A.9. The full front-axis steering system will be modeled around the cylinder.

OSPS Hydraulic System

In this section, the directional valve which consists of a spool and a sleeve will be modeled. As shown in Figure A.10 the proportional valve is described as a function of inner orifices areas that will open and close depending on the valve's angular position.

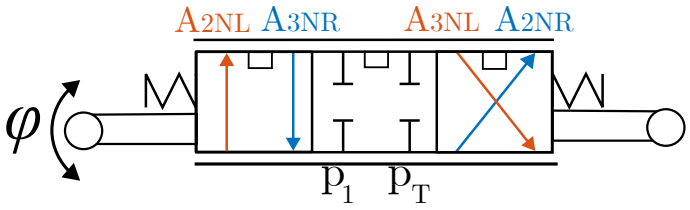

Figure A.4. *Valve model showing it being dependent on* φ*.*

Therefore, Figure A.4 will be modeled as a series of orifices that depend on φ*. Figure A.5 shows the orifices of the simplified proportional valve mode.*

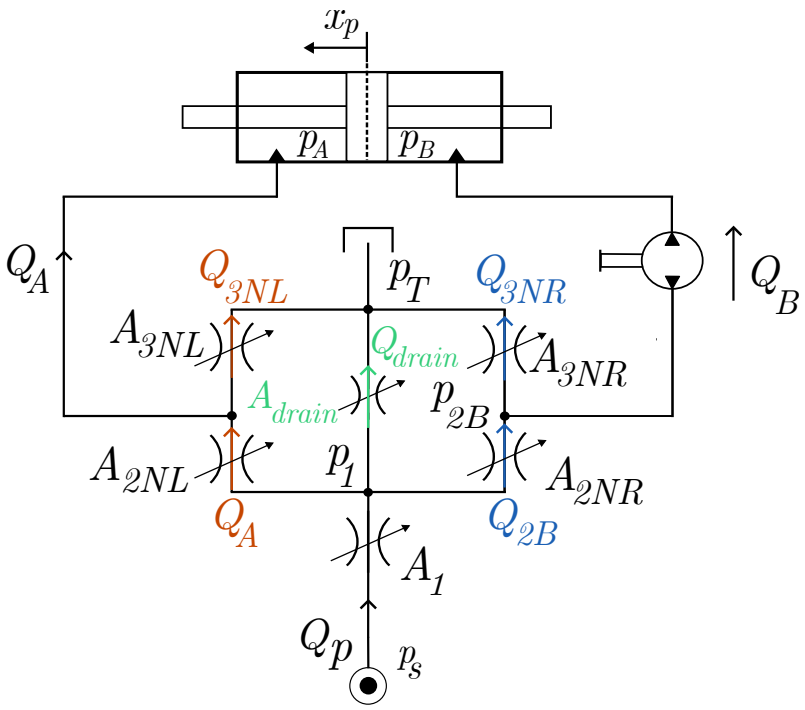

Figure A.5. *Model how the orifice areas are connected in the valve.*

The area characteristics of $A_1, A_{2NL}, A_{2NR}, A_{3NL}, A_{3NR}, A_{drain}$ are provided by Danfoss. These are mapped below in Figure A.6 where the area is normalised between fully closed and fully open. A_1, acts as the connection between the system and the supply pump, and is always open to keep the pressure required by the system when actuated. To keep the pressure level for actuation in the OSPS when in neutral a flow is needed since the system otherwise would see an increasing pressure. This flow is achieved via A_{drain}. The areas A_{2NL} and A_{2NR} acts as openings from supply to cylinder chambers. A_{3NL} and A_{3NR} opens from the cylinder chambers to the tank.

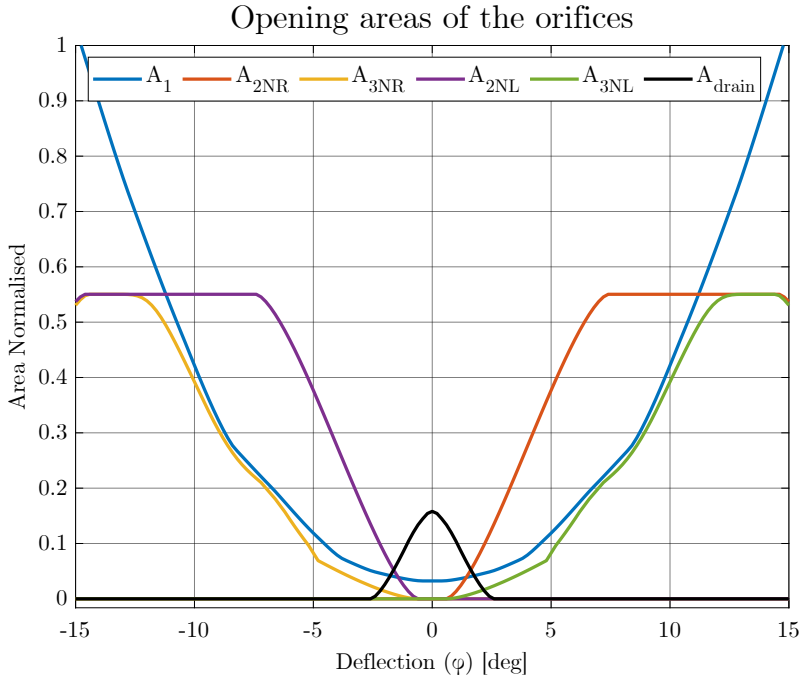

Figure A.6. *Areas as a function of the deflection angle φ [2].*

The opening areas depend on φ. The area of the orifices given in Figure A.6.

$$Q(\varphi) = k_v\, A_d(\varphi)\, \sqrt{|\Delta p|}\, sign(\Delta p) \tag{A.8}$$
$$k_v = C_d \sqrt{\frac{2}{\rho}}$$

Where C_d is the discharge coefficient, ρ is the density of the working fluid, A denotes the opening area as a function of φ, Q is the actual flow and Δp is the pressure difference.

$$Q_p = k_v\, A_1(\varphi) \sqrt{\Delta p_{s,1}} \tag{A.9}$$

The hydraulic system functions such that p_S will always be 15 bar *larger than p_1. To ensure this the orifice equation for Q_p will be defined such that the pressure difference, $\Delta p_{s,1}$, is always* 15 bar*. The rest of the flow is described as Equation* (A.10) *to Equation* (A.14)*.*

$$Q_A = k_v\, A_{2NL}(\varphi) \sqrt{|p_1 - p_A|}\, sign(p_1 - p_A) \tag{A.10}$$
$$Q_{2B} = k_v\, A_{2NR}(\varphi) \sqrt{|p_1 - p_{2B}|}\, sign(p_1 - p_{2B}) \tag{A.11}$$
$$Q_{3NL} = k_v\, A_{3NL}(\varphi) \sqrt{|p_A - p_T|}\, sign(p_A - p_T) \tag{A.12}$$
$$Q_{3NR} = k_v\, A_{3NR}(\varphi) \sqrt{|p_{2B} - p_T|}\, sign(p_{2B} - p_T) \tag{A.13}$$
$$Q_{drain} = k_v\, A_{drain}(\varphi) \sqrt{|p_1 - p_T|}\, sign(p_1 - p_T) \tag{A.14}$$

The flow Q_B seen on the right side of Figure A.5 is through the gear set. This gear set functions as a hydraulic motor and is modeled based on [4] and can be seen in Equation (A.15)*:*

$$Q_B = D_{\dot{\theta}_{SL}} \dot{\theta}_{SL} + C_{Le1}(p_{2B} - p_B) - C_{Le2}(p_B - p_T) \tag{A.15}$$

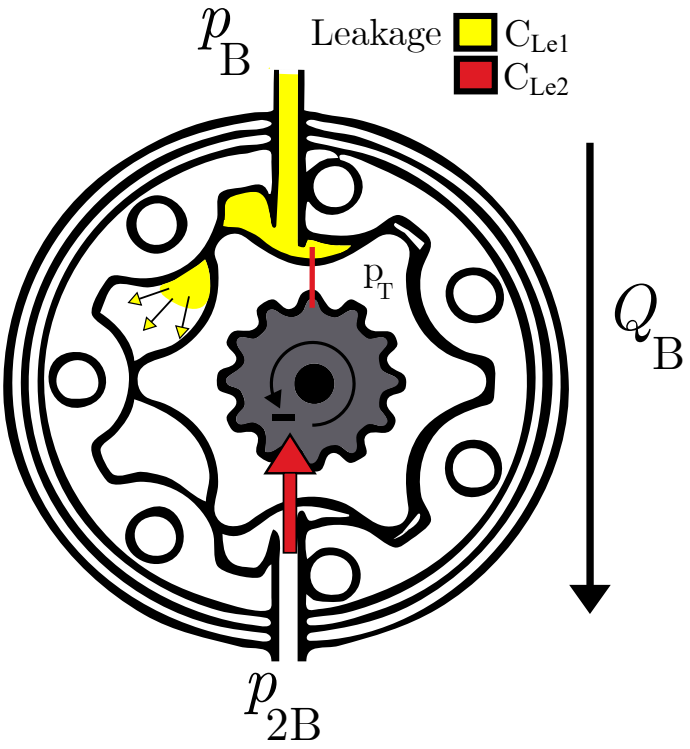

Figure A.7. *Showing flow through gear set and how leakage occurs.*

As seen in Equation (A.15) *and Figure A.7 there is leakage over the gear set. The leakage is split into two parts, one is caused due to tolerances between components when they interface. This causes the leakage C_{Le1} to go from the high-pressure side to the lower-pressure side therefore following the flow direction of Q_B. The other leakage C_{Le2} is to tank and therefore is a negative contribution to Q_B.*

Pressure Gradients In The Valve

Using the general continuity equation of a cylinder chamber gives Equation A.16:

$$Q_{in} - Q_{out} = \dot{V} + \frac{V}{\beta_{eff}}\dot{p} \tag{A.16}$$

Q_{in} and Q_{out} is the flow into and out of the control volume defined as V, $\dot{V}$ is the volume change, $\dot{p}$ is the pressure gradient and β_{eff} is the bulk modulus of the working fluid.

$$\dot{p}_1 = \frac{\beta_{eff}}{V_1}\left(Q_p - Q_A - Q_{2B} - Q_{drain}\right) \tag{A.17}$$

$$\dot{p}_{2B} = \frac{\beta_{eff}}{V_{2B}}\left(Q_{2B} - Q_{3NR} - Q_B\right) \tag{A.18}$$

The pressures in relation to the hydraulic system can be seen in Figure A.5.

Pressure Gradients In The Hydraulic Cylinder

Here the equations describing the pressure build-up in the cylinder chambers will be explained. The pressures and the flows can be seen in Figure A.8

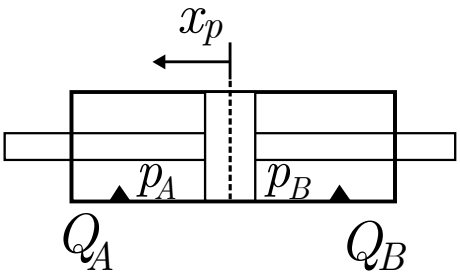

Figure A.8. *Steering cylinder showing pressure and flow into and out of the chambers*

The volume of the cylinder chamber and the hoses are dependent on the displacement of the cylinder.

$$V = V_d + A\,x_p + A\,\frac{x_{max}}{2} \tag{A.19}$$

V_d is the dead volume in the hoses, A is the area of the cylinder and x_p is the displacement of the cylinder. $A\,\frac{x_{max}}{2}$ is used to define the middle of the cylinder as the zero point.
The flow gradients are derived for each flow into and out of the chamber via Equation (A.16).

$$\dot{p}_A = \frac{\beta_{eff}}{V_{DA} + A_A\,\frac{x_{max}}{2} - A_A\,x_p}\,(Q_A + A_A\dot{x}_p - Q_{3NL}) \tag{A.20}$$

$$\dot{p}_B = \frac{\beta_{eff}}{V_{DB} + A_B\,\frac{x_{max}}{2} + A_B\,x_p}\,(Q_B - \dot{x}_p A_B) \tag{A.21}$$

With the pressure gradients disclosed the pressure in the cylinder chambers can be found.

Forces on the Cylinder

The forces acting on the cylinder can now be considered utilizing Newton's second law as seen in Equation (A.22). *This is where all the forces from the system are gathered in the model. Thus the mass will be the mass of the entire front axis, including the mass of the rims.*

$$\ddot{x}_p m_{axis} = F_{hyd} - F_{fric} - F_{tires} \tag{A.22}$$

With m_{axis} being the mass of the front axis F_{hyd} being the hydraulic forces acting on the cylinder, F_{fric} being the friction in the cylinder, and F_{tires} being the load forces from the tires acting on the cylinder. These forces are given as seen in Equations (A.23) *to* (A.25)

$$F_{hyd} = p_A\,A_A - p_B\,A_B \tag{A.23}$$

The friction is described in Equation (A.24).

$$F_{fric} = B_{cyl}\,\dot{x}_p + F_{cyl}\,sign(\dot{x}_p) \tag{A.24}$$

With B_p being the viscous friction constant, and F_c being the coulomb friction constant.

$$F_{tires} = F_{Ltire} + F_{Rtire} \tag{A.25}$$

”

A.1.3 Additional Information

The naming of Figure A.5 has been changed as can be seen in Table A.1, this is to more easily differentiate between reaction mode orifices and operating orifices. The result of this can be seen in Figure 4.2. This means that:

[1] naming	Naming in this project
Q_A	Q_{2A}
Q_{3NL}	Q_{3A}
Q_{3NR}	Q_{3B}

Table A.1. Change in naming convention

Furthermore Equation (A.25) is included in the model. However, as this project focuses on the hydraulic OSP system the steering geometry and thus the tire forces are not disclosed, these can be found in [1] from page 14 to 22.

The citation from Appendices A.1.1 and A.1.2 refers to 2 figures in an earlier Chapter in [1]. These figures (Figures A.9 and A.10) can be found in [1] on page 2 and 3 respectively, they are a direct citation and will be shown here:
“

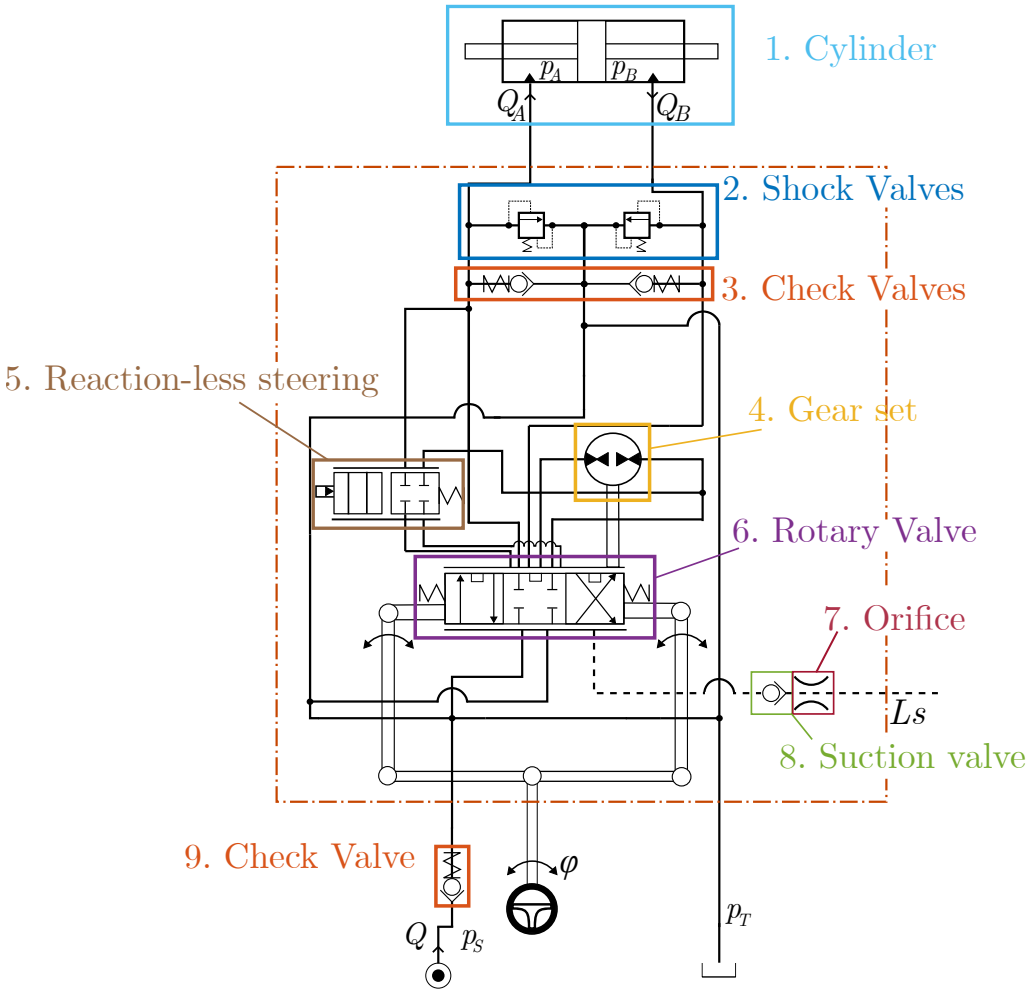

Figure A.9. *Hydraulic diagram of an OSPS 315.*

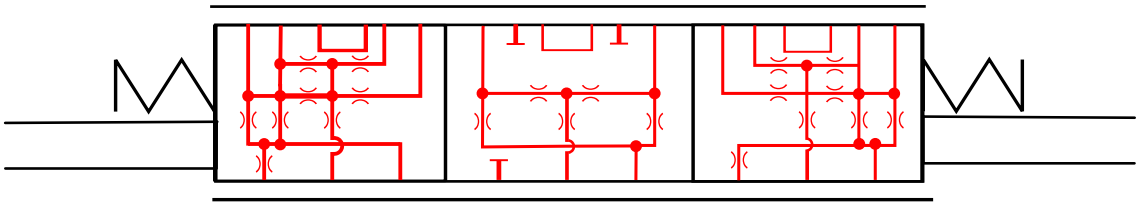

Figure A.10. *Rotary valve overview.*

”

A.2 Enlarged Figures

These are figures throughout the report that could use a larger view for better understanding. These figures are in the report and the original figure is referred to in the caption.

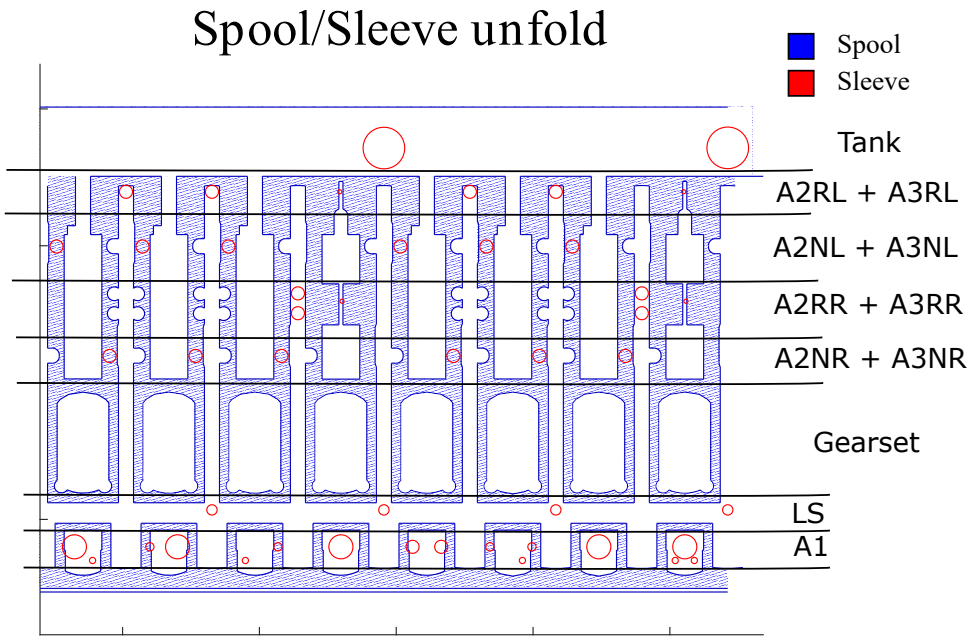

Figure A.11. Figure 2.7

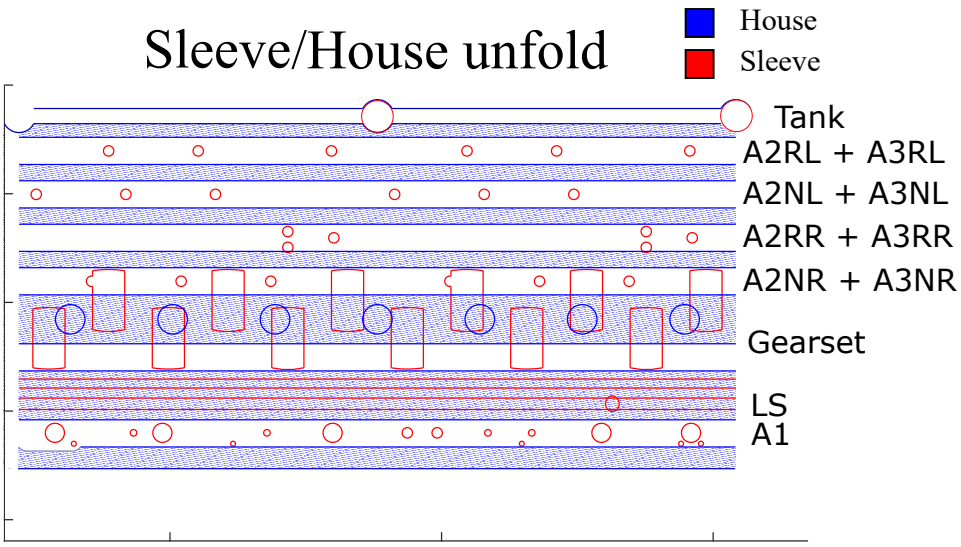

Figure A.12. Figure 2.8

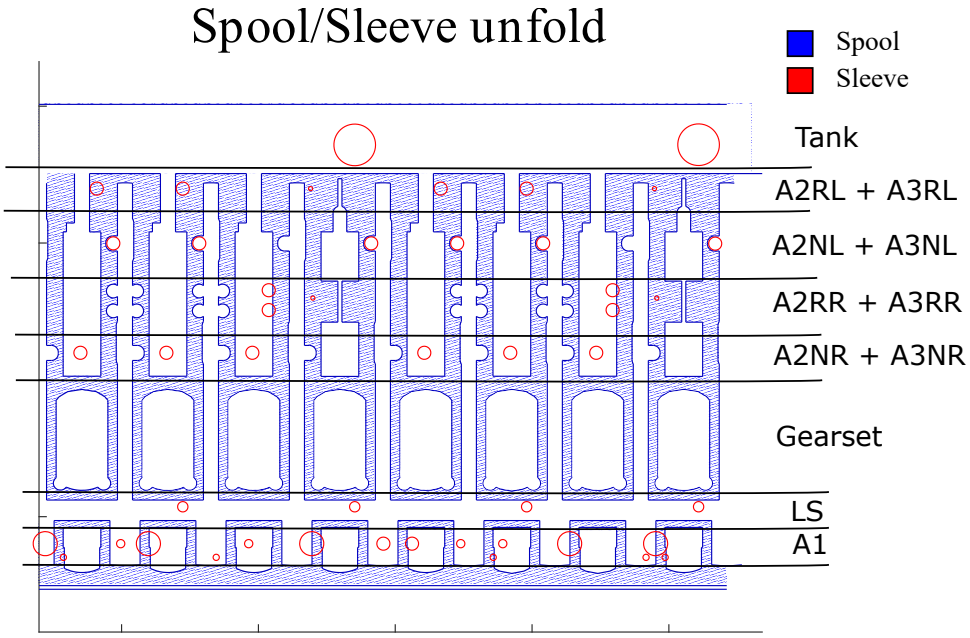

Figure A.13. Figure 2.9

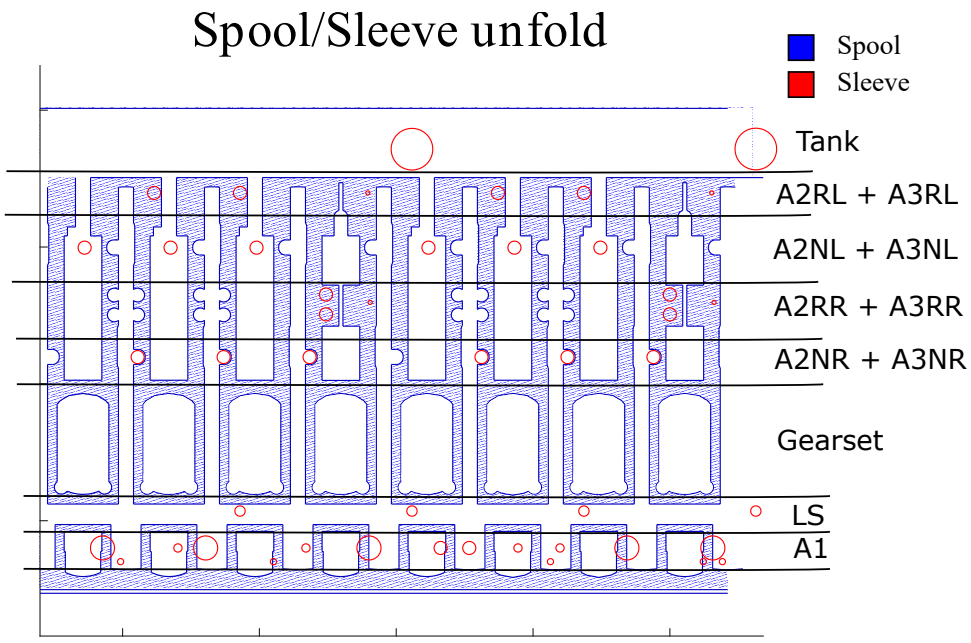

Figure A.14. Figure 2.10